Elaf Ali Hadi Jarallah

Characterization of DHA-induced stress response in colorectal cancer cells with focus on autophagy

Master of Science in Pharmacy

Trondheim, June 2018

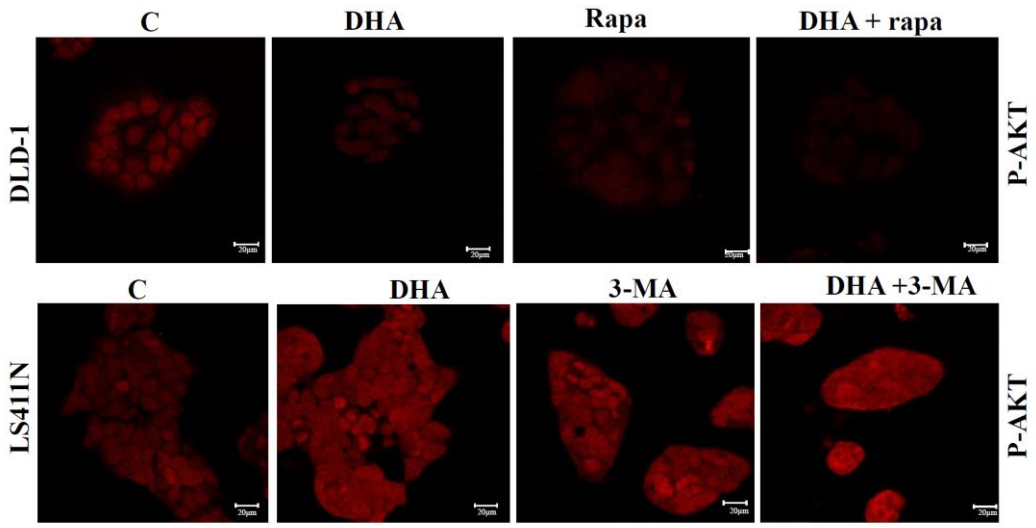

NTNU
Norwegian University of
Science and Technology

Contents

Acknowledgements vi
Abstract viii
List of abbreviations x
1. **Introduction** 1
1.1Fatty acids 1
1.1.1 Classification, structure, and nomenclature 1
1.1.2 Biosynthesis of fatty acids 2
1.1.3 Uptake and transport of fatty acids 3
1.1.4 Polyunsaturated fatty acids 3
1.1.5 Daily intake recommendations of EPA and DHA 3
1.1.6 Mechanism and functions of n-3 PUFAs 4
1.2 Cancer 5
1.2.1 Carcinogenesis 5
1.2.2 Hallmarks of cancer 6
1.2.2 Colorectal cancer 9
1.2.3 Treatment of CRC 9
1.3 Cancer and PUFAs 10
1.3.1 Anticancer properties of PUFAs 10
1.4 Autophagy 12
1.4.1 Mechanism and function 12
1.4.2 Regulation 15
1.4.3 The PI3K/AKT pathway 15
1.4.4 The mTOR Pathway 17
1.5 Aim of study 18
2 Method 19
2.1 Cell culture 19
2.1.1 Cell lines 19
2.1.2 Thawing, cell culturing and cell treatments 19
2.2 Cell counting 20
2.3 Gene expression 20
2.3.1 Data analysis 20
2.4 Cell harvesting and protein isolation 21
2.4.1 Protein isolation 21
2.4.2 Protein quantification 21
2.5 Western Blotting 22

2.5.1 Preparation of samples 22
2.5.2 Gel electrophoresis 22
2.5.3 Blotting 22
2.5.4 Blocking, hybridization and detection 23
2.5.5 Quantification of the data 24
2.6 Confocal Microscopy 24
2.6.1 Fixation 24
2.6.2 Permeabilization, blocking, staining and imaging 24
2.7 Flow Cytometry 26
2.7.1 Autophagy level measured by Cyto-ID and flow cytometry 26
3. Results 27
3.1 Four different CRC cell lines respond differently to DHA treatment 27
3.2 Gene expression levels are associated with DHA sensitivity 27
3.3 Differences in the basal level of autophagy in untreated CRC cells 28
3.4 DHA sensitivity is associated with the level of autophagy 29
3.4.1 Microscopic imaging shows that CRC cells respond differently to DHA 31
3.5 DHA treatment affects autophagy level to different extent in CRC cell lines 33
3.6 DHA increased the level of the autophagy marker protein MAP1LC3BII in DHA sensitive CRC cells 37
3.7 DHA affects AKT signaling in both DHA sensitive and less DHA sensitive CRC cell lines 38
3.8 Confocal imaging indicates differences in the effect of DHA on p-AKT protein expression 42
3.9 DHA treatment has different effect on p-mTOR expression in DHA sensitive and less DHA sensitive CRC cells 45
4. Discussion 51
4.1 DHA induced different growth response in four human CRC cell lines 51
4.2 Gene expression level of autophagy-related genes differ between DHA sensitive and less DHA sensitive cell lines 52
4.3 The basal level of autophagy is associated with the degree of DHA sensitivity 53
4.4 Induction of autophagy reduced DHA sensitivity in CRC cells 53
4.5 Inhibition of autophagy increased DHA sensitivity 55
4.6 DHA treatment affected the AKT signaling pathway in both DHA sensitive and less sensitive CRC cell lines 55
4.7 DHA treatment affected the expression level of p-mTOR in different ways in DHA sensitive and less DHA sensitive CRC cell lines 57
4.8 Troubleshooting the western blotting procedure 58
5. Conclusions and future perspectives 61
References 63
Appendix 69

Appendix A: Chemicals and equipment 69
Appendix B: Buffers and solutions used during protein isolation and western blotting 70
Appendix C: Protein ladders 71
Appendix D: Buffers and antibody solutions during immunofluorescent staining 72
Appendix E: Buffers and solutions used during flow cytometry 72

Acknowledgements

This study is the result of the research related to my Master's Thesis, performed at The Department of Clinical and Molecular Medicine, Children's and Women's Health, Norwegian University of Science and Technology (NTNU) during the years 2017-2018.

There are a lot of people that deserve credit for this work. There is no doubt that without these colleagues, family and friends, this accomplishment would not have been possible.

I would first like to thank my supervisor Professor Svanhild Schønberg for your guidance and advices during the entire length of this project. Thank you for allowing me to be a part of your research group.

I would also thank my co-supervisor Caroline Hild Pettersen, for your patience and support. Thank you for all the time you have spent reading the thesis. Thank you for always being there for me even in the busiest of times.

I am grateful to Therese Stork Høiem for helping me through the laboratory work and Helle Samdal for helping and teaching me with western blot and spent time reading the thesis.

Finally, I must express my gratitude to my family, especially my parents, for their passionate support and motivation.

Trondheim, June 2018

Elaf Ali Hadi Jarallah

Abstract

The modern western diet contains a high amount of omega-6 (n-6) polyunsaturated fatty acids (PUFAs) compared to omega-3 (n-3) PUFAs. Many studies have indicated that docosahexaenoic acid (DHA; 22:6 n-3) can inhibit cancer cell growth both *in vivo* and *in vitro*. Several mechanisms have been suggested to mediate the cytotoxic effect of n-3 PUFAs like alteration of prostaglandin synthesis, oxidative stress and lipid peroxidation, alterations in membrane composition, as well as transcription factors involved in signaling pathways like autophagy and the integrated stress response in cancer cells. Studies by our group have previously and recently shown that DHA induces ER stress and growth arrest in some human colorectal cancer cell lines. The aim of this thesis was to identify the molecular mechanisms involved in the anticancer properties of DHA in four human colorectal cancer cell lines, grown in the same culture medium, with special focus on basal autophagy level and the autophagy-regulating AKT-mTOR pathway.

Four colorectal cancer cell lines, DLD-1, HCT-8, LS411N, and LS513 cells, responded differently to DHA (70 μM) treatment. All four cell lines were grown in the same growth medium. The effect of DHA on cell growth was estimated by cell counting, showing that DLD-1 and HCT-8 cells were sensitive to DHA (70 μM, 48 h) treatment with a growth inhibition of approximately 45 % and 25 % for DLD-1 and HCT-8 cells, respectively. LS411N and LS513 cells showed almost no growth inhibition given the same conditions. The basal level of autophagy and the level of protein MAP1LC3BII were found to be higher in the less DHA sensitive cell lines (LS411N and LS513) compared to DHA sensitive cell lines (DLD-1 and HCT-8). Gene expression analysis indicated an association between the level of DHA sensitivity and autophagy. DHA in combination with an autophagy inducer, rapamycin, decreased DHA sensitivity in DLD-1 and HCT-8 cells, while co-treatment with an autophagy inhibitor, 3-MA, increased the DHA sensitivity in LS411N and LS513 cells. Flow cytometry and the cyto-ID probe were used to assess the autophagic structures in the cells. The results indicated an increase in autophagic flux and the protein level of MAP1LC3BII in DLD-1 and HCT-8 cells after co- treatment with rapamycin and DHA, compared to rapamycin. In the LS411N and LS513 cells, the autophagic flux and level of MAP1LC3BII were found to decrease after co- treatment with 3-MA and DHA compared to 3-MA alone. The gene expression data indicated a possible connection between the AKT/mTOR pathway and the degree of DHA sensitivity in CRC cell lines. The p-AKT and p-mTOR levels decrease in DLD-1 and HCT-8 cells, indicating that the DHA-induced autophagy in DLD-1 and HCT-8

cells was possibly regulated by the AKT/mTOR pathway. Co-treatment with 3-MA and DHA was observed to increase the p-AKT and p-mTOR levels by confocal imaging, indicating a possible inhibition in autophagy level in LS411N and LS513 cells.

Some of the results presented in figures 10 B, 15, and18 is recently published in FEBS Journal [1].

List of abbreviations

AA	arachidonic acid
AKT/PKB	protein kinase B
AMPK	AMP-activated protein kinase
APC	adenomatous polyposis coli
ATG	autophaghy-related genes or proteins
ATF6	activating transcription factor 6
CoA	coenzyme A
COX	cyclooxygenase
COX-2	cyclooxygenase-2
CO2	carbon dioxide
CRC	colorectal cancer
DHA	docosahexaenoic acid
DMSO	dimethyl sulfoxide
DTT	dithiotreitol
eIF2α	eukaryotic translation initiation factor 2
ER	endoplasmic reticulum
ERAD	endoplasmic reticulum-associated protein degradation
EtOH	ethanol
FA	fatty acid
FAS	fatty acid synthase
HNF-4α	hepatocyte nuclear factor 4 alpha
HNPCC	hereditary nonpolyposis colorectal cancer
IRE1α	inositol-requiring enzyme 1 alpha
LA	linoleic acid
LOX	lipoxygenase
LPO	lipid peroxidation
MeOH	methanol
mTOR	mammalian target of rapamycin
mTORC1	mammalian target of rapamycin complex 1
MAP1LC3B	microtubule-associated protein 1 light chain 3β
N-3	omega-3
N-6	omega-6
NADPH	nicotinamide adenine dinucleotide phosphate

NF-κB	nuclear factor NF kappa B
PBS	phosphate buffered saline
PE	phosphatidylethanolamine
PERK	protein kinase RNA-like ER kinase
PFA	paraformaldehyde
PGE2	prostaglandin E2
PI3K	phosphatidyl inositol-3 kinase
PIP3	phosphatidyl inositol-3 phosphate
PPAR	proliferator-activated receptor
PUFA	polyunsaturated fatty acid
RAS	rat-sarcoma family of genes
ROS	reactive oxygen species
RXR	retinoid X-receptor
SREBP	sterol regulatory element binding protein
TAG	triacylglycerol
TBS	tris buffer saline
TBST	tris buffer saline with tween
TGFβ	transforming growth factor beta
TP53	tumor suppressor protein p53
TSC1	tuberous sclerosis 1
TSC2	tuberous sclerosis 2
ULK	atg1/unc-51- like kinase
UPR	unfolded protein response
WHO	World Health Organization

1. Introduction

The modern western diet contains a high amount of omega-6 (n-6) polyunsaturated fatty acid compared to omega-3 (n-3) PUFAs, with an n-6 PUFAs to n-3 PUFAs ratio about 25:1. An increased n-6: n-3 ratio, have been found to affect the pathogenesis of many diseases, including cancer and inflammatory diseases. Many epidemiological studies have found that there is a strong association between nutrient composition of the diet and colorectal cancer. The amount of total dietary fat is important, and the type of fat has been shown to play a significant role. Intake of fish oil and oily fish have also been associated with the protection against development of some cancer types, including colorectal cancer. Some studies have shown that fatty acids and monounsaturated fatty acids may have a weak effect on promoting tumor growth. Both *in vivo* and *in vitro* studies have indicated that n-3 PUFAs can inhibit cancer cell growth. Several mechanisms have been suggested to mediate the cytotoxic effect of n-3 PUFAs like alteration of prostaglandin synthesis, oxidative stress and lipid peroxidation, alterations in membrane composition, as well as transcription factors involved in signaling pathways like autophagy and integrated stress response in cancer cells [2, 3].

1.1 Fatty acids

1.1.1 Classification, structure, and nomenclature

Fatty acids (FAs) contain a hydrocarbon chain of variable length, with a methyl group (CH_3) at one end and a carboxyl group (-COOH) at the other end (n or ω-end). The carbon chain is bound together by single and/or double bond. FAs are classified as saturated fatty acids (SFAs) and unsaturated fatty acids (UFAs). FAs have single bonds completely saturated with hydrogen atoms, while UFAs are further divided into monounsaturated fatty acids (MUFAs) and polyunsaturated fatty acids (PUFAs), which are not saturated with hydrogen atoms. The n-3 and n-6 families are the most common PUFAs in nature, in which the first double bound is located either 3 or 6 carbons from the n-end, respectively [4].

Nomenclature of the FAs can be reached by using the International Union of Pure and Applied Chemistry (IUPAC) recommendations. This system applies several characteristics of the FAs including the number of carbon atoms, and the number and positions of double bonds to establish the proper nomenclature. The IUPAC name of α- linolenic acid is *cis*, *cis*, *cis*-

9,12,15 octadecatrienoic acid or (ALA). The most common system is the C: D (n minus) system, where C is the number of carbon atoms in the chain and D is the number of double bonds. The n minus system refers to the position of the first double bond closest to the methyl end of the FA chain. Exemplified, by using AA (n-6, 20:4) and docosahexaenoic acid (DHA, 22:6, n-3) and eicosapentaenoic acid (EPA, 20:5, n-3, fig.1 [5]).

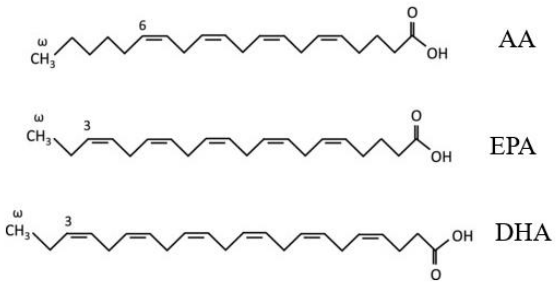

Figure 1: Chemical structures and nomenclature of arachidonic acid (AA), DHA and EPA (copied from[6]).

1.1.2 Biosynthesis of fatty acids

Carbon atoms from the energy source (generally carbohydrates) will be converted to FAs, mainly in the liver and in lactating mammary glands, where they are stored as TAGs. The synthesis of FAs starts by breaking down the carbohydrates into acetate units. In the FA synthase (FAS) complex the carbons from acetyl coenzyme A (CoA) is combined with series of malonyl CoA to form palmitate. This is an energy requiring process using adenosine triphosphate (ATP). FAS uses malonyl-CoA as a carbon donor, adding two carbon units to synthesize the palmitic acid (16:0) [7].

Elongases and desaturases are enzymes that are responsible for the elongation and desaturation of FAs. Elongation takes place in smooth ER (SER) by adding two carbon units to make longer FAs where malonyl CoA is the donor and NADPH supplies the electrons, a process aided by the action of different enzymes. Desaturases use O_2 and NADPH to introduce double bonds into the FA chain. In the human body, the desaturases are not able to introduce double bonds between carbon atoms beyond carbon C-9. For that reason, linoleic acid and ALA are essential in the diet [7, 8].

1.1.3 Uptake and transport of fatty acids

The free fatty acids (FFA) and monoacylglycerols are released and absorbed in the small intestine. The FFA are re-esterified to TAGs in the intestinal mucosa and transported through lymphatic vessels before they enter the blood stream as part of chylomicrons. FAs are carried in plasma and bound to albumin, as part of lipoproteins. FAs are transported into the cells, with help of FA transporters (FATs) where they are taken up by FA binding proteins (FABPs). FAs may be converted in the cell to the activated form, fatty acyl-CoA (FA-CoA) to mitochondria and may be exposed to β-oxidation, and may also be elongated and desaturated [9].

1.1.4 Polyunsaturated fatty acids

N-3 PUFAs, n-6 PUFAs, and n-9 PUFAs, are important PUFAs in human diet and health. The fatty acids ALA, linoleic acid (LA 18:2, n-6) and oleic acid (OA, 18:1, n-9). These fatty acids have to be provide by the diet. ALA is found at high levels in green leafy vegetables, flaxseed and, walnuts. LA is found mostly in plant oils, like safflower, grape seed, hemp, corn and soybean. While DHA and EPA are rich in seafood, fatty fish and fish oil (FO). The efficacy of the alteration of ALA to EPA or DHA becomes low at preterm birth and may decrease with age [10]. DHA and EPA have been shown to influence coronary heart disease, rheumatoid arthritis, and brain function. DHA has also been reported to be effective in slowing down the rate of cognitive decline, while its effects on depression disorders are still unclear [11].

1.1.5 Daily intake recommendations of EPA and DHA

Recommended intake of EPA and DHA are normally given as a total of these FAs since they occur together in food sources. The World Health Organization (WHO) and Food and, Agriculture Organization (FAO) and the European Food Safety Authority (EFSA) recommend a daily intake of EPA and DHA at 250 mg, whereas the American Dietetic Association and American Heart Association recommend an intake of approximately 500 mg/day. The Japanese Ministry for Health recommends as much as 1000 mg/day. However, the daily intake of EPA and DHA in most of the world is significantly lower than 500 mg/day [12]. A decrease in EPA and DHA incorporated into cellular membranes is associated with an increase in AA that may have negative impact on human health [10]. The Nordic Nutrition Recommendations (NNR) for *cis*-MUFAs is 10-20% of total energy intake. For other FAs

they recommended intake of SFAs should be <10 E%, and cis-PUFAs should be 5-10 E% including at least 1 E% as n-3 PUFAs [13].

1.1.6 Mechanism and functions of n-3 PUFAs

Studies have shown that n-3 and n-6 PUFAs have important functions in maintaining structure and function of cell membrane. They also play important role in signaling and regulation of gene expression. In additional, they act as substrates for energy production via β-oxidation and serve as energy stores as part of triacylglycerols (TAGs) [14].

Membrane fluidity increases with the amount of n-3PUFAs incorporated into the membrane phospholipids. The different physical characteristics of the membrane may affect the function of different membrane proteins and affected signaling pathways. Eicosanoids are important signaling molecules derived from AA, EPA, and docosanoids, derived from DHA [14].

One group of n-3 PUFA derived eicosanoids are resolvins. It has been shown that resolvins have potent anti-inflammatory effects. The resolvins are primarily derived from DHA and EPA. The D series of resolvins are metabolite of DHA and E-series from EPA [2].

The synthesis of eicosanoids starts with the release of AA or EPA from glycerol in the membrane by the enzyme phospholipase A_2. EPA and AA may be metabolized by either cyclooxygenase (COX) or lipoxygenase (LOX). The COX pathway leads to the formation of prostaglandins and thromboxanes, while the LOX pathway leads to formation of leukotrienes. AA metabolized by COX undergoes conversion into prostaglandin E_2 (PGE_2), which is an pro-inflammatory mediator, while prostacyclin I_2 (PGI_2) is responsible for blood vessel dilation and thromxane A_2 (TXA_2) activating blood platelet aggregation [7]. Metabolism of n-3 and n-6 PUFAs is summarized in fig. 2.

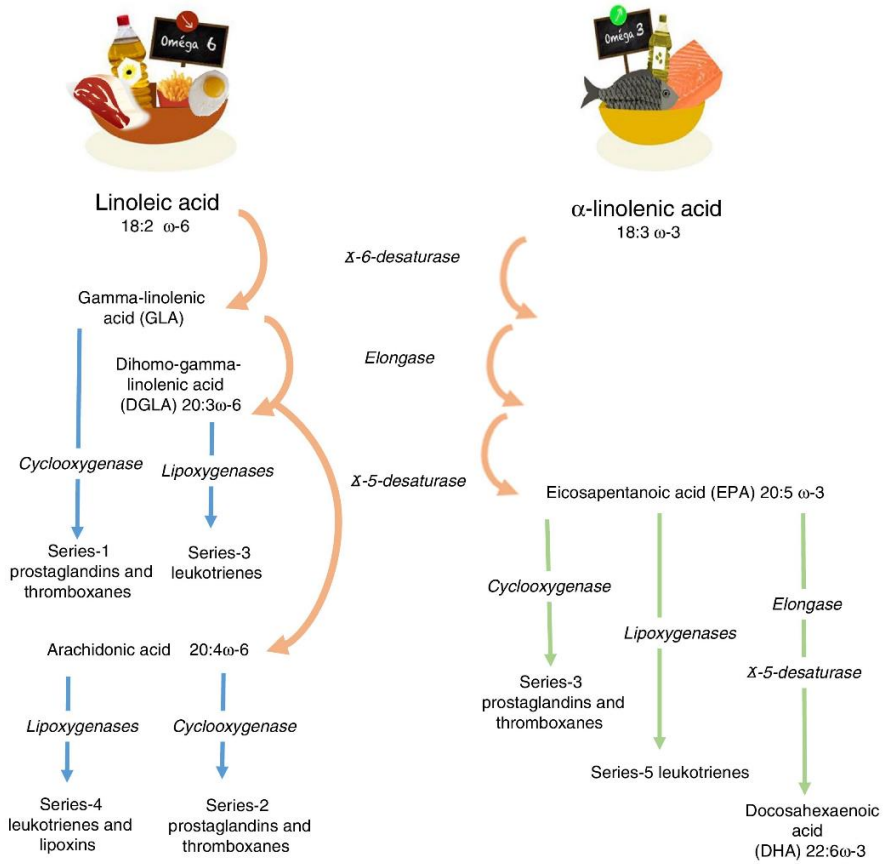

Figure 2: Metabolism of LA and ALA (the figure is adapted with permission from [15])

1.2 Cancer

1.2.1 Carcinogenesis

In 2012 there were about 14.1 million cancer cases worldwide. Of these cases 7.4 million were in men and 6.7 million in women. The number is expected to increase to 24 million by 2035. Cancer is the second leading cause of death globally and was responsible for 8.8 million deaths in 2015 [16].

Cancer is a group of diseases characterized by uncontrolled cell proliferation. Cancer cells have the potential to spread to and invade any tissues and organs. The abnormalities in cancer cells are a result of mutations in protein-encoding genes [17].

Carcinogenesis is the process where normal cells are transformed into cancer cells. The process can be divided into four steps: tumor initiation, tumor promotion, malignant conversion and tumor progression (fig. 3). Carcinogenesis is a complex process and involves mutational actions causing the inactivation of tumor suppressor genes and the activation of protooncogenes. Cancer occurs by a series of successive mutations in genes leading to changes cell functions [18].

Cancer cells are part of a tumor microenvironment that includes both transformed and non-transformed cancer cells, like immune cells and vascular endothelial cells. Normal cells both grow and divide, but they only grow when stimulated by growth factors, in contrast to cancer cells that are much less dependent on growth signals [19].

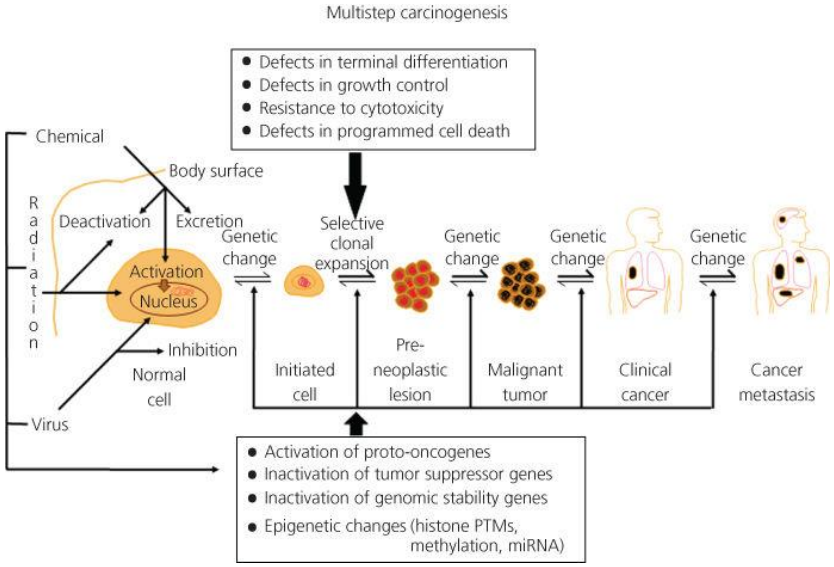

Figure 3: Multistep process of carcinogenesis. During these steps, epigenetic changes are also occurring due to chemical exposure (The figure is copied from [20]).

1.2.2 Hallmarks of cancer

Hanahan and Weinberg have described the hallmarks of cancer, that enable tumor growth and metastatic spreading, for better understanding of the biology of cancer fig. 4.

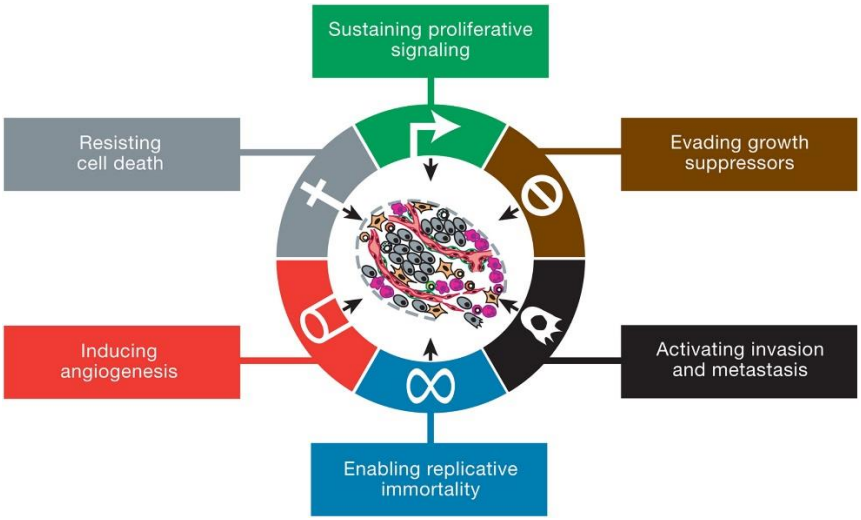

Figure 4: Summary of some essential alterations in cell physiology that contribute to malignant growth (the figure is copied from [21]).

Sustaining proliferative signaling

Cancer cells can divide for an unlimited number of times. Normal cells are dependent on growth signals to activate a proliferative state, in contrast cancer cells are independent on growth signals. Cancer cells may produce their own growth signals, thereby stimulate their own proliferation through a positive feedback mechanism. One mechanism to sustain the proliferative signaling is by increasing the number of receptors to growth factors on the cell membrane (reviewed in [21]).

Evading growth suppressors

Cancer cells are resistant to growth suppressor mechanisms duo to mutations in the genes responsible. Two important tumor suppressors, retinoblastoma protein (RB) and tumor protein 53 (TP53), are often found mutated in cancer. RB regulates cell cycle progression from G1 and S phase. In normal cells, if the stress level becomes too high, TP53 can stop further cell cycle progression. Cancer cells are able to evade growth suppression because of the loss- of function of these regulators (reviewed in [21]).

Resisting cell death

Cell death by apoptosis is a program that is activated in response to many physiologic stresses in cancer cells. Apoptosis is composed of both upstream regulators and downstream effector components. TP53 induces apoptosis, and loss of TP53 is a common strategy that cancer cells

evolve. Other strategies to avoid cell death by apoptosis are induction of autophagy, antiapoptotic regulators (Bcl-2, Bcl-x_L), the extrinsic ligand-induced death pathway and downregulating proapoptotic factors (reviewed in [21]).

Activating invasion and metastasis

Invasion and metastasis are complex multistep processes, starting with local invasion of the cells into the neighboring tissues. Cancer metastasis is the spread of cancer cells to tissues and organs beyond where the tumor originated from and the formation of new tumors. Increased expression of E-cadherin is well-known as an antagonist of invasion and metastasis (reviewed in [21].

Inducing angiogenesis

Angiogenesis is the physiological process through which new blood vessels form from pre-existing vessels. All cells need oxygen and nutrients, as well as removal of metabolic waste and CO_2. Angiogenesis is turned on as part of physiological processes, like wound healing and female reproductive cycling. An angiogenic switch is almost always activated and remains on during tumor progression. There are different inducers and inhibitors regulating this switch, like vascular endothelial growth factor-A (VEGF-A) and thrombospndin-1 (TPS-1) (reviewed in [21]).

Replicative immortality

Cancer cells require unlimited replicative potential in order to generate macroscopic tumors, while normal cells can only pass through a limited number of division before entering senescence or crisis. Immortalization is reached when cells emerge from a population in crisis that have the potential to unlimited replication. The limited proliferation in normal cells is caused by the shortening of their telomerase. Cancer cells have an increased telomerase activity. Telomerase is an enzyme that is able to elongate the telomeres. In normal cells this enzyme is inactivated, but in cancer cells telomerase is activated, which results in reduced induction of senescence and crisis (reviewed in [21]).

Hanahan and Weinberg suggest some new hallmarks; reprogramming of energy metabolism and evading immune destruction, tumor-promoting inflammation and genome instability and mutation. The cancer reprograms the metabolism to improve is support to neoplastic growth. Cancer cells have increased rates of mutations, caused by an increased sensitivity to mutagens or a fault in the genomic maintenance system. Most tumors have been found to contain

immune cells in variable numbers. This is considered to be a challenge of the immune system to combat the disease, but the inflammatory effect has also been found to promote tumor growth (reviewed in [21]).

1.2.2 Colorectal cancer

Colorectal cancer (CRC) is one of the main causes of cancer death in both men and women. CRC is the third most common type of cancer worldwide, with about 1.4 million new cases diagnosed in 2012. 54% of all CRC cases are found in established countries. In 2012 CRC caused 700.000 deaths, even with progress in early diagnosis/screening, surgery, and chemotherapy [22]. In 2016 there were 1588 and 1415 new cases of CRC respectively for women and men in Norway, and CRC is considered the fourth main type of cancer in the country [23].

It is known that many risk factors, such as genes and environmental factors, are involved in malignant transformation. CRC is mostly due to lifestyle, especially obesity and physical inactivity are associated with increased risk, but also dietary factors such as red meat, tobacco and alcohol [15].

Hereditable gene mutations, which increase the risk of CRC can be accumulated in families. It has been found mutations that increase the risk of CRC in the mismatch repair genes, which lead to Lynch syndrome, also known as hereditary nonpolyposis colorectal cancer (HNPCC). People with HNPCC have a tendency to develop colon cancer before the age of 50. Another common form of inherited CRC syndrome is familial adenomatous polyposis (APC). Some reviews have concluded that CRC are one of the most genetically complex cancers. Common driver mutation, include mutations in APC, rat sarcoma family of genes (RAS), phosphatidyl inositol 3-kinase (PI3K), and transforming growth factor beta (TGFβ), are either tumor-suppressor genes or proto-oncogenes [24].

1.2.3 Treatment of CRC

The treatment of CRC is based on stage of the disease and the subtype of the tumor. Clinical staging of CRC is used to regulate the size of tumor cancer and involves the use of the Tumor Node Metastasis (TNM) staging system [25]. The existing therapy forms are mainly surgery and radio- and chemotherapy. Surgery is the primary treatment for CRC and used to treat

individuals with stage I or stage II CRC. 5- Fluorouracil (5-FU) and oxaloplatin are the most commonly used chemotherapeutic drugs to treat CRC. 5-FU has been commonly used for stage III colon cancer and stage III rectal cancer. 5-FU based chemotherapy is the typical cytostatic in the adjuvant treatment of CRC, and the most effectively to reduce tumor recurrence [26].

5-FU has a fluorine atom at the C-5 position in place of hydrogen, and the drug is an analog of uracil. The mechanism of action of 5-FU is through the inhibition of thymidylate synthase and the combination of its active metabolites, fluorodeoxyuridine monophosphate (FdUMP), fluorodeoxyuridine triphoshphate (FdUTP) and fluorouridine triphosphate (FUTP) into RNA and DNA to influence the uracil metabolism. FdUMP, an active metabolite is incorporated into RNA to replace uracil and inhibit cell growth. Moreover, FdUTP inhibits thymidylate synthetase, depleting thymidine triphosphate, and eventually induces to apoptosis in the cancer cells [26, 27].

5-FU has a low response when giving it as first line monotherapy. Therefore, it is given in combination with other cytotoxic agents, like oxaliplatin and irinotecan. 5-FU is normally given either as a bolus injection with leucovorin, which favors RNA damage, or a continuous infusion favors DNA damage [28].

1.3 Cancer and PUFAs

1.3.1 Anticancer properties of PUFAs

Several experimental studies have explored the effects of n-3 PUFAs and n-6 PUFAs on CRC [15]. Many factors can be involved in the development of CRC, and genetics is an important risk factor. Furthermore, some epidemiological and experimental studies have suggested that the consumption of Western-style diet, high in fat and proteins, significantly increases CRC risk [29]. Moreover, a high intake of fruits, vegetables, and whole grains may protect against CRC development [30]. The anticancer effect of n-3 PUFAs have also been documented in several studies, both *in vitro* and *in vivo*. Some experimental and clinical studies have concluded that DHA can be used in the management of some types of cancer and that it increases the response to anticancer therapy, including some chemotherapeutic drugs like 5-FU and tamoxifen, photodynamic therapy and radiation [31].

PUFAs effect gene expression

The cellular and molecular mechanisms mediating the anticancer effect of n-3 PUFAs are complex. Several studies have shown that PUFAs interact with peroxisome proliferator-activated receptors (PPARs), the hepatocyte nuclear factor (HNF)-4α, the retinoid X receptor (RXR) alpha, sterol regulatory element-binding proteins (SREBP's) and the nuclear factor kappa-light-chain-enhancer of activated B cells (NF-κB) [30]. DHA inhibits the activation of NF-κB, leading to reduction in the production of pro-inflammatory eicosanoids from cyclooxygenase-2 (COX-2) and decreased the production of cancer promoting cytokines induced by NF-κB [30].

COX-modulation and resolvin production

Some studies have demonstrated that n-3 PUFAs can inhibit the anti-apoptotic COX-2/PGE2 pathway in tumor cells, thus leading to cancer cell apoptosis. Since PGE_2 has a pro-inflammatory activity, stimulates platelet aggregation, and serves as a vasoconstrictor, it seems to play a role in the early stages in colorectal carcinogenesis. The metabolism of DHA and EPA by LOX and aspirin-modified COX enzymes, also produces resolvins, which have been shown to have anti-inflammatory activity. The anti-inflammatory effect of the resolvins may also suppress carcinogenesis, as inflammation is recognized as one of the emerging hallmarks of cancer. DHA is able to inhibit the activity of COX-2, when found overexpressed in colon cancer [32].

N-3 PUFAs increase oxidative stress in tumor cells

One characteristic of n-3 PUFAs is that they are substrates for oxidants inside the cell and are highly inclined to lipid peroxidation (LPO) because of their double bonds. Their integration into phospholipids of cellular membranes may sensitize cells to reactive oxygen species (ROS) and thereby induce oxidative stress. Cancer cells have higher levels of ROS compared to normal cells, due to their faster metabolism needed to maintain their high proliferation rate. N-3 PUFAs are easily peroxidized, which increases intracellular ROS levels and oxidative stress in tumor cells. Furthermore, it is known that ROS can oxidize and inhibit factors in key signaling pathways, like MAPK and NF-κB pathway, which are involved in cell proliferation, survival and apoptosis (reviewed in [32]).

Endoplasmic reticulum stress

The main functions of Endoplasmic Reticulum (ER) is to maintain Ca^{2+} homeostasis, biosynthesis of lipids and sterols, synthesis of membrane- and secretory proteins and protein folding. When these functions are disturbed, ER stress is induced and causing accumulation of unfolded or misfolded proteins in the ER lumen, followed by activation of the Unfolded Protein Response (UPR). The UPR is an adaptive cell response and when activated functions as a cytoprotective mechanism, to overcome ER stress by upregulation of relevant chaperones. There are three different ER stress sensor-proteins that are associated with the UPR, PKR-like ER kinase (PERK), inositol requiring kinase 1 (IRE1α) and activating transcription factor 6 (ATF6). Activation of the ER stress pathway results in attenuation of protein synthesis to avoid further accumulation of unfolded proteins, and transcriptional induction of ER chaperone genes to increase the cell's folding capacity, as well as transcriptional induction of the ER-associated degradation (ERAD) component genes to help the destruction of aberrant proteins [33].

The environment in tumors is low in pH, hypoxic and low in nutrients, and these factors may induce ER stress. Many cancers have adapted different strategies to avoid ER stress associated cell death, which make the UPR a potential target in anti-cancer therapy [34]. Jakobsen *et al* (2008). have shown that DHA induces ER stress, UPR and growth arrest in several human cancer cell lines. They found an increased protein levels of PERK-mediated phosphorylation of elF2α, at early time points [35]. They also found that the expression of ER-stress related genes are upregulated in the colon cancer cell line SW620 after treatment with DHA, like ATF6, PERK and ATF4 [36].

1.4 Autophagy

1.4.1 Mechanism and function

Lately, it has been shown that induction of ER stress as well as many other forms of cellular stress like nutrient deprivation, ROS, DNA damage, protein aggregates and damaged organelles induce autophagy [36]. Macroautophagy (referred as autophagy hereafter) plays a key role in both normal tissue homeostasis and tumor development. It is also necessary for cancer cells to adapt efficiently to a negative tumor microenvironment, which is characterized by hypo nutrient environments [37].

Autophagy is a catabolic process that is characterized by cellular self-digestion. Autophagy breaks down damaged and redundant cellular components, which are recycled and used as nutrient and energy to maintain the cell's integrity and stability. Autophagy arises as a physiological process in normal cells at a basal level. The process is important, because it protects organisms against diverse pathologies, including infections, cancer, neurodegeneration, aging and heart disease. Both *in vitro* and *in vivo* studies have shown the importance of autophagy in many diseases, including colorectal cancer. The word autophagy is originating from two Greek words ''auto and phagia'' which means ''to eat oneself''[38]. There are three types of autophagy, macroautophagy, microautophagy and chaperone-mediated autophagy. Macroautophagy means the presence of double membrane vesicles known as an autophagosome vacuoles that engulf cellular macromolecules and relaxed organelles, leading to their breakdown after fusion with lysosomes.

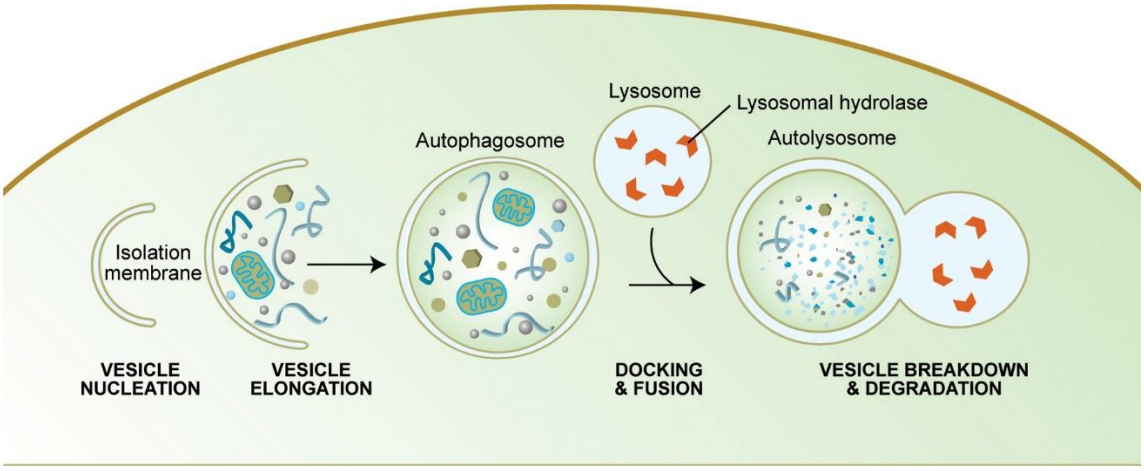

Figure 5: Degradation of cellular content by macroautophagy (the figure is copied from [39]).

Autophagy starts with an isolation membrane, also known as a phagophore. The phagophore derives from a lipid bilayer contributed by ER, the trans-Golgi apparats and endosomes [40]. The phagophore increases in response to intra-cellular cargo, like protein aggregates, organelles and ribosomes, in that way sequestering the cargo in a double-membrane autophagosome. The overloaded autophagosome develops through fusion with the lysosome, helping the degradation of autophagosomal contents by lysosomal acid proteases. Then the lysosomal permeases and transporters export amino acids and other by-products of the degradation back out to the cytoplasm, where they can be re-used for building new macromolecules as shown in fig.5 [41].

It has been discovered more than 30 different autophagy-related genes (ATG). ATG genes encode proteins involve in all steps of the autophagy process, like initiation, vesicle formation, fusion of the autophagosome with the lysosome, and degradation of the cargo. These genes also encode proteins for the release of the degradation products into the cytosol, to be broken down by the cell [42]. ATGs are activated, when cells receive signals of starvation or of intracellular stress. The activity of the autophagy related 1 (Atg1) kinase in a complex with Atg13 and Atg17 is essential for phagophore creation in yeast, probably by regulating the recruitment of the transmembrane protein Atg9 that may act help lipid employment to the expanding phagophore [43]. This is regulated by the target of rapamycin (TOR) kinase that phosphorylates Atg13, thereby avoiding it from interacting with Atg1.

Microtubule-associated proteins 1A/1B light chain 3B (MAP1LC3BI/II) are the mammalian homologues of the Atg8 encoded gene product in yeast. The unprocessed form of LC3B is sliced by Atg4 protease, resulting in the LC3B-I form with a carboxyterminal exposed glycine. The exposed glycine of LC3B-I is conjugated by Atg7, Atg3 and Atg12-Atg5-Atg16 to generate a phosphatidylethanolamine(PE)-conjugated form, LC3B-II. PE promotes integration of LC3B-II into the lipid membrane of the phagophore and autophagosomes. LC3B-II is the most well-characterized protein that is localized to autophagic structures through the process from phagophore to lysosomal degradation as shown in fig.6 [44].

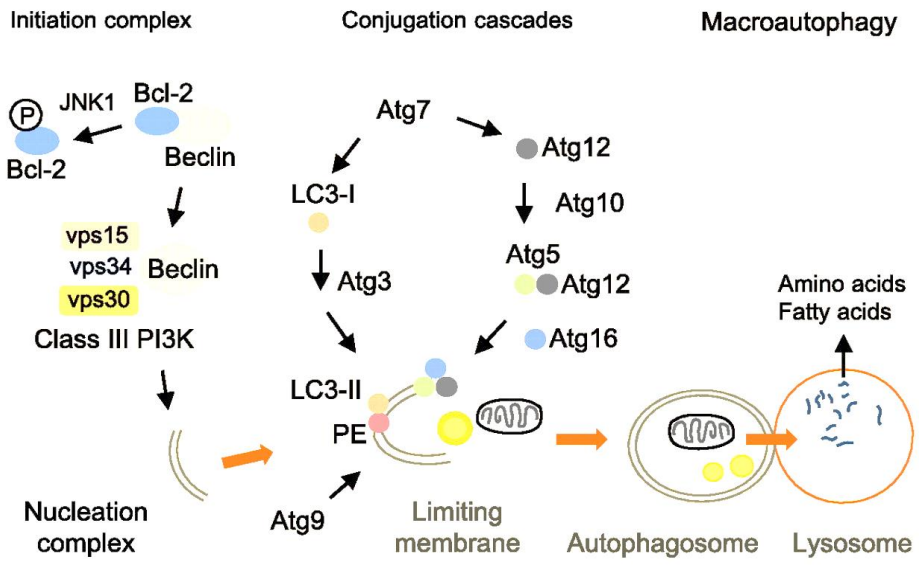

Figure 6: Molecular constituents of autophagy (the figure is copied from [45])

1.4.2 Regulation

Autophagy has dual roles in cancer, and it can act as both a tumor promoter and a tumor suppressor. In normal cells autophagy acts to protect cells from malignant changes by removing damaged organelles and aggregated proteins. Furthermore, autophagy reduces DNA damage, ROS and mitochondrial abnormalities. But it also promotes tumor development by providing increased amounts of nutrients, increasing drug resistance and inhibiting cell death [46]. If autophagy is highly accelerated or down regulated, leading to too much or too little autophagy, respectively, the process may act toxic. Up regulation of autophagy may result in the inability of the cells to survive due to degradation of cytoplasmic components, and uncontrolled up regulation of autophagy can activate apoptosis [47].

Several pathways have an important role in making sure that the autophagic machinery function correctly. mTOR have a central point in autophagy regulation. Upstream regulators of mTOR are therefore, relevant in the regulation of autophagy, like the Phosphatidylinositol-3kinases (PI3K)/protein kinase B (AKT/PKB) pathway.

1.4.3 The PI3K/AKT pathway

The PI3K/AKT pathway is a key regulator of survival after cellular stress. The PI3Ks are a large family of lipid enzymes. There are three classes of PI3Ks (class I, class II and class II), which have been identified in mammals [48]. Class I PI3Ks contain a catalytic subunit p110 and a regulatory subunit p85. Activation of PI3Ks is induced by activated growth factor receptor tyrosine kinases. When PI3K is activated, it catalyzes the conversion of phosphatidylinositol 3,4,5 trisphosphates (PIP3) by phosphorylating PIP_2, thereby recruiting a subset of signaling proteins with Pleckstrin homology (PH) domains to the membrane, including other signaling proteins such as protein serine/threonine kinase-3'-phosphoinositide-dependent kinase 1 (PDK1) and AKT (reviewed in [49]).

AKT plays a key role in autophagy because of its critical role in regulating diverse cellular functions, as well as metabolism, growth, proliferation, survival, transcription, and protein synthesis. The AKT signaling cascade starts by receptor tyrosine kinases, integrins, B and T cell receptors, cytokine receptors and G-protein-coupled receptors that induce production of PIP3 by PI3K. PDK1 phosphorylates AKT at Thr308 leading to partial activation of AKT. Phosphorylation of the serine residue at position 473 (Ser743) of AKT, lead to full activation of AKT [49, 50]. mTOR has been shown to phosphorylate this residue when mTOR is

complexed with rictor, an insensitive rapamycin agent [51]. Activation of the PI3K/AKT pathway is illustrated in fig.6.

Some inhibitors of PI3K, like 3-methyladenine (3-MA) and wortmannin, have been commonly used as autophagy inhibitors based on their inhibitory effect on class III PI3K activity. Class III PI3K is known to be essential for induction of autophagy. Wu *et al* (2010) found out that 3-MA blocks class I PI3K, while its suppressive effect on class III PI3K is temporary. Therefore, the autophagy promotion activity of 3-MA is due to its differential temporal effects on class I and class III PI3K [52].

Wortmannin can also inhibit class I PI3K. The wortmannin has antitumor action both *in vivo* and *in vitro* studies. Further, studies in animal models have been used to test the efficacy of wortmannin in inhibiting tumor growth *in vivo*. These studies propose that blocking the PI3K/AKT pathway with wortmannin may be a valuable method to treat cancer. One weakness of the use of wortmannin is its stability in an aqueous environment. Wortmannin is soluble in organic solvents, thus makings it less usable in clinical trials [53].

Dysregulation of the PI3K/AKT pathway is implicated in many human diseases, including cancer [54]. In cancer, two mutations that increase the intrinsic kinase activity of PI3K, have been discovered. Furthermore, phosphatase and tensin homlog (PTEN) is a tumor suppressor that often found mutated in human tumors [50].

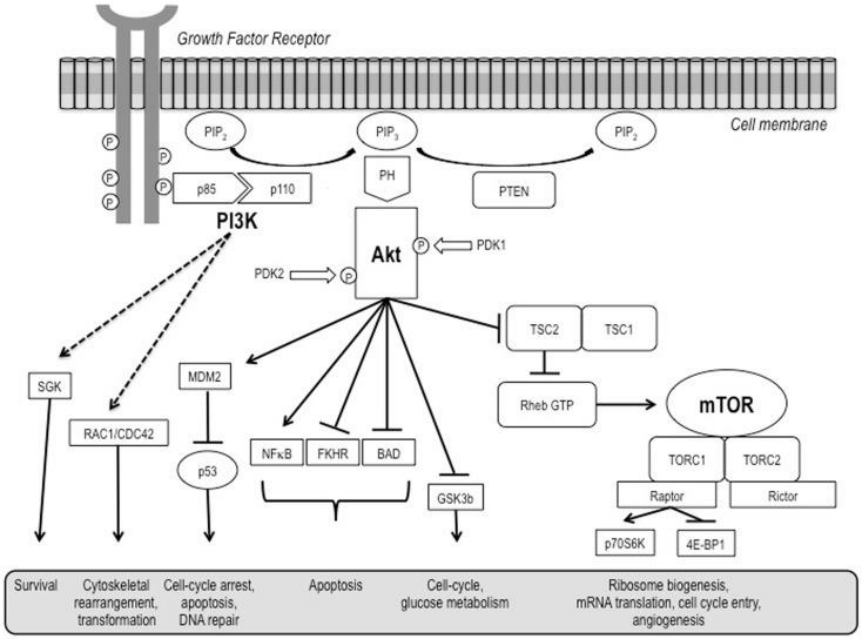

Figure 7: Schematic presentation of the PI3K/AKT/mTOR pathway (the figure is copied from [49])

1.4.4 The mTOR Pathway

The mTOR pathway is a key regulator of cell growth and proliferation and is involved in many disease states, including colorectal cancer, cardiovascular disease, and diabetes [51]. AKT phosphorylates Tuberous sclerosis complex 2 (TSC2), destabilizes it and disrupts its interaction with Tuberous sclerosis complex 1 (TSC1), leading to activation of mTOR. mTOR is found in two complexes that regulate growth and metabolism. mTOR complex 1 (mTORC1) found in mammals and contains mTOR, G protein beta protein subunits-like, GβL (mLST8), a proline- rich AKT substrate of 40 kDA (PRAS40), Raptor, and DEPTOR. mTORC1 is sensitive to inhibition by rapamycin. mTORC1 is a negative regulator of autophagy by inhibitory phosphorylation of ULK1 [55]. Stimulation of autophagy starts with inactivation of mTORC1 by rapamycin. mTORC1 is a growth regulator that senses and integrates diverse nutritional and environmental signals, as well as growth factors, energy levels, cellular stress, and amino acids. It combines these signals to the promotion of cellular growth by phosphorylating substrates that activate anabolic processes like mRNA translation and lipid synthesis or limit catabolic processes such as autophagy [56].

The TSC1/TSC2 are the major upstream inhibitory regulators of mTOR. TSC2 consists a GAP homology domain and stimulates GTP hydrolysis of Ras homolog enriched in brain (Rheb). GTPase Rheb is necessary and effective stimulator of mTORC1 kinase activity. TSC1 works as a GTPase-activating protein for Rheb, therefore TSC2 inhibits Reb activity [56]. The second mTOR complex is mTORC2, which is consists of mTOR, Rictor, GβL, Sin1, PRR5/Protor-1 and DEPTOR. mTORC2 promotes cellular survival by activating AKT, regulated cytoskeletal dynamics by activating PKCα [57, 58].

Autophagy may be inhibited by high glucose and insulin- induced PI3K signaling via AKT/PKB and mTOR. mTOR kinase is blocked by signals that sense nutrient deprivation, including hypoxia [59]. mTOR can be inhibited by treatment of cells with rapamycin (also known as sirolimus). Rapamycin is a macrolide, an antifungal agent and has immunosuppressive and anticancer properties [60]. It has been shown that inactivation of mTOR, induces autophagy, whereas activation of mTOR is able to inhibit autophagy [43]. The complex pathway from activation of PI3K to inhibition of autophagy by mTOR is illustrated in fig.7 and 8.

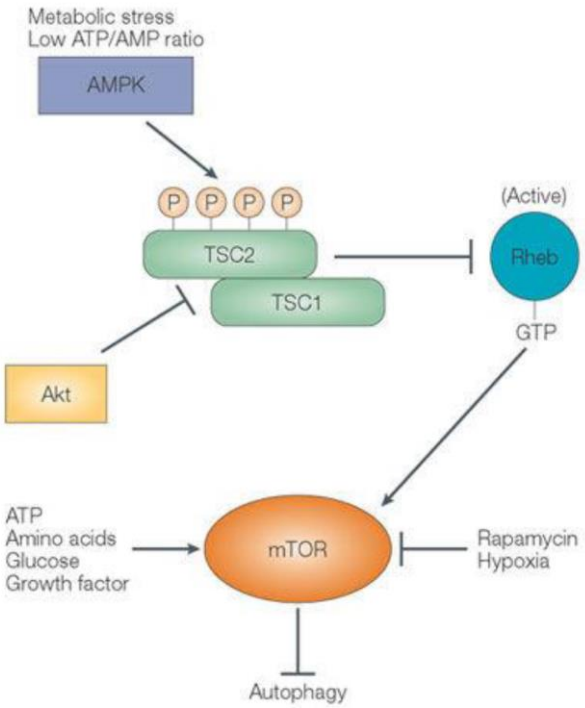

Figure 8: The mTOR signaling pathway. mTOR signaling regulates critical cellular processes. Arrows represent activation, bars represent inhibition (copied from[61]).

1.5 Aim of study

Previous work by our group showed that colorectal cancer cell lines respond differently to treatment with the omega-3 fatty acid, DHA, and suggests that the level of basal autophagy is important for DHA sensitivity in colorectal cancer cells. The aim of this study was to identify the molecular mechanism involved in the anticancer properties of DHA in human colorectal cancer cell lines representing different CRC subtypes, grown in the same culture medium, with special focus on basal autophagy level and the autophagy-regulating AKT-mTOR pathway.

2 Method

2.1 Cell culture

2.1.1 Cell lines

LS411N is a colorectal carcinoma cell line isolated in 1985 from a primary tumor biopsy of a Dukes' type B. LS513 is a colorectal carcinoma cell line establishes from a primary tumor biopsy of a Dukes' C. DLD-1 initiates from a Dukes' type C human colon adenocarcinoma. HCT-8 initiates from an ileocecal colorectal adenocarcinoma. The four cell lines were obtained from the American Type Culture Collection (ATCC, USA). The cells were stored in an N_2-container.

2.1.2 Thawing, cell culturing and cell treatments

- **Thawing**

The four cell lines were thawed in a water bath (37°C) for five minutes. The cells were resuspended in 9 ml growth medium, before centrifugation at 125 g for 7 minutes. The supernatant was discarded to remove DMSO from the cryoprotective media. Next, the cell pellet was re-suspended in 11 ml preheated growth medium and transferred to a 75 cm^2 flask. The flask was incubated at 37 °C and 5% CO_2.

- **Cancer cell line culturing**

All four cell lines were maintained in Roswell Park Memorial Institue (RPMI, England)1640 medium supplemented with 10% fetal bovine serum (FBS, Gibco, England) and gentamicin (0,5%, Gibco Life Technology, England). The cell lines were cultured in 175 cm^2 cell culture flasks and incubated at 37°C in an incubator with 5% CO_2 and humidified atmosphere. All solutions used were preheated in a water bath (37°C). During cell sub cultivation, the growth medium was discarded, and the cells were washed with phosphate saline buffer (PBS 2 x 10ml). After washing, the cells were detached using trypsin (2.5 ml) with ethylene diamine tetraacetic acid (EDTA, USA) for 8-10 minutes. The cells were re-suspended in fresh growth medium, counted using the Moxi Z cellcounter (Orflo technologies) and added to new culture flasks.

- **Cell treatments**

Cells were treated with DHA (70 µM, Sigma-Alderich, USA). Other treatments were used; Ethanol (EtOH) as control, (Rapa 50 nM), DMSO (50nM), (3-MA 3mM), and combinations DHA+ Rapa or DHA + 3-MA. Treatments were added to growth medium to get the wanted concentration by using a 10 µL syringe and/or a pipette. The supplemented media was vortexed for 30 seconds and incubated in water bath (37°C) for 20 minutes. Then the medium was removed from the cell culture flasks and substituted with supplemented media.

2.2 Cell counting

The effect of DHA and the other treatments was investigated by cell counting 24 and 48 h hours after treatment. Cells were seeded in 12 well plates. 24 h after the cells were seeded, the growth medium was removed and growth medium supplemented with treatments were added. 24 and 48h after supplementation, the growth medium was discarded, the cells were washed with PBS (2 x 1 ml) and detached from the wells using trypsin (0.2 ml) for 8-10 min, before re-suspended in growth medium (1 ml). The effect of the different treatments was measured by cell counting using Moxi z mini automated cell counter (ORFLO Technologies, USA) S type cassette.

2.3 Gene expression

Gene expression profiling of the four cell lines have been performed at our research group, previously. Cells were harvested 48 h after seeding. RNA was isolated from the cells using High Pure Isolation Kit (#11828665001, Roche). Expression analysis was done in duplicate experiments by using Human Genome U133 Plus 2.0 array from Affymetrix (Santa Clara, LA, USA) and the Genchip system.

2.3.1 Data analysis

Gene expression raw data are registered in the Array Express database with accession number E-MTAB-5750. Gene expression analysis was supported by Lene C. Olsen at Bioinformatics core facility- BioCore, IKOM, NTNU. Analysis of the microarray data was conducted in R (version 3.2.2). The expresso function in the Affy Bioconductor package for background

correction (rma method) and normalization (quantile) was used. The Limma Bioconductor package was used for differential expression analysis. The duplicateCorrelation function to handle the correlation between technical replicates was used. Statistical significance was assessed by testing if the regression coefficient in samples sensitive to DHA treatment was equal to one. The p-values were adjusted for multiple testing using a Benjamini-Hochberg correction with a threshold of 0.05 and summarized in a gene list.

Differently expressed probes from indicated categories were chosen from the gene list.

2.4 Cell harvesting and protein isolation

DLD-1 and HCT-8 cells were seeded in 155 cm^2 plates, and LS411N and LS513 cells were seeded in 55cm^2 plates. The cells were incubated for 24 h at 37°C and 5% CO_2 before the growth medium was switched with supplemented growth medium containing EtOH, DHA (70 µM), 3-MA (3 mM), rapamycin (50 nm), or a combination of two of these treatments. Cells were incubated and harvested after 3, 6, 12 and 24 h. As a control of DHA sensitivity, cell counting experiments were performed parallelly with cell harvesting for protein analysis.

2.4.1 Protein isolation

The medium was removed from the plates. The cells were washed with cold PBS (2 x 10 ml for 155 cm^2 plates) and (2 x 4 ml for 55cm^2 plates). The cells were scraped in 7ml cold PBS for the big plates and 5 ml for the small plates, transferred to a 15 ml tube and centrifuged at 2000 rpm (4 C°) for 10 min. The supernatant was discarded before the pellets were re-suspended in 1 ml cold PBS and transferred to cold Eppendorf tubes. The suspension was centrifuged once more at the same setting. Urea lysis buffer (Appendix B) was added to the pellets, before vortexing for 30 seconds and incubating on ice for 30 seconds. This was repeated three times before centrifuged at 4 °C for 15 min at 13 000 rpm. The supernatant was transferred to new cold Eppendorf tubes, snap frozen in liquid N_2 and stored at -80°C.

2.4.2 Protein quantification

Protein concentration were measured using BioRad protein assay. A mixture of Biorad concentrated solution (BioRad laboratiories, USA) and Milli Q (MQ) water was diluted in a

ratio of 1:5. Three parallels from each protein extract were made by adding 1µl sample to 999µl diluted Biorad, and urea lysis buffer was used as blank. The samples were then incubated for 20 min before measured on the spectrophotometer at 595 nm. The protein concentration for each sample was calculated with the help of the measured absorbance and a standard curve, as shown in Formula 1.

Protein concentration (µg/µl) = *Absorbance* 595 x 22.02 x *dilution* **Formula 1**

2.5 Western Blotting

2.5.1 Preparation of samples

The protein samples were thawed on ice and centrifuged before diluted in Tris- HCl-(10mM, pH 8.0) buffer to have the same protein concentration in all samples. A mix of NuPAGE LDS buffer (Life technologies, USA) and dithiothreitol (DTT, Sigma Aldrich, USA) were added to the samples. Prepared samples contained 70% diluted proteins, 25% NuPAGE LDS 4x sample buffer and 5% DTT. Odyssey protein molecular weight marker (928-40000, LI-COR biosciences, USA) was used. The samples were heated (80 °C for 15 min), centrifuged and loaded onto the gel.

2.5.2 Gel electrophoresis

4-12% NuPAGE™ Invitrogen Bis-Tris 10- or 12 well gel (Life technologies) were used. The gels were run in Xcell SureLock Mini-cell (Life Technologies). NuPage MOPS SDS running Buffer was added the inner and outer chamber of the Mini-Cell. The proteins were separated at 200 V for 50 min at room temperature.

2.5.3 Blotting

The gels were transferred to Immobilion Transfer Membranes (Merch Millipore, USA) in the XCell™ blot module according to the NuPage technical guide and placed in the XCell SureLock™ Mini-Cell as recommended by the supplier. Transfer buffer from NuPAGE was filled into the middle chamber, and the outer chamber was filled with cold dH_2O. The blotting was carried out at 30 V for 60 min at room temperature.

2.5.4 Blocking, hybridization and detection

The membranes were rehydrated in methanol (MeOH, 20 seconds) and Tris Buffered Saline with tween (TBST) or phosphate buffer saline with tween (PBST) for 20 seconds. The protein side of the membrane was facing in, when transferring the membrane to a 50 ml tube with 4 ml blocking solution (5 g dry milk (5%) and 100 ml of PBST or TBST) and incubated on roller at room temperature for 1 hour.

The primary antibodies (table 1) were centrifuged and diluted in 4 ml TBST + dry milk solution. The membranes were incubated with primary antibody solution in cool room on rolling overnight. The membranes were rinsed once in 5 ml TBST (Appendix B) and washed with 5 ml TBST for 3 x 10 min. Secondary antibodies (table 2) were diluted in milk solution and added to the 50 ml tubes containing membranes, and incubated for 1 h at room temperature in a dark room, because of the light-sensitivity of the secondary antibodies. The membranes were washed with 5ml TBS for 3x10 min and dried in an open box in the dark closet, approximately 1 h, before imaging using Odyssey Infared imaging System (Li-cor Biosciences, UK).

Table 1: Primary antibodies used for protein staining in western blotting experiments.

Antigen	Primary antibody	Manufacturer	Dilution
AKT	mouse monoclonal	Cell Signaling 4060#29675	1:1000
β-actin	mouse monoclonal	Abacam Ab6276	1:5000
LC3BII	rabbit monoclonal	Cell Signaling 3868S	1:500
m-TOR	mouse monoclonal	Fisher Scientific (215Q18)	1:1000
P-AKT	rabbit monoclonal	Cell signaling 4060	1:500
P-mTOR	rabbit monoclonal	Cell signaling Ser2448	1:500

Table 2: Secondary antibodies used for protein staining in western blotting experiments.

Antigen	Secondary antibody	Manufacture	Dilution
AKT anti mouse	IRDye 800 CW donkey anti mouse IgG	Licor Odyssey	1:10000
Mouse anti β-actin	IRDye 700 CW conjugated donkey anti mouse IgG	Licor Odyssey	1:10000
LC3BII anti rabbit	IRDye 700 CW conjugated donkey anti rabbit IgG	Licor Odyssey	1:10000
m-TOR anti mouse	IRDye 700 CW conjugated donkey anti mouce IgG	Licor Odyssey	1:10000
P-AKT anit rabbit	IRDye 700 CW conjugated donkey anti rabbit IgG	Licor Odyssey	1:10000
P-mTOR ani rabbit	IRDye 800 CW conjugated donkey anti rabbit IgG	Licor Odyssey	1:10000

2.5.5 Quantification of the data

The image Studio version 3.1 was used to quantify the bands signals from the membranes. The signals were normalized to their respective loading control and fold change values of treated samples versus controls were calculated. Excel software 2016 was used to calculate significance indicated by P-value below 0.05, using students t-test (paired, one tiled).

2.6 Confocal Microscopy

2.6.1 Fixation

Cells were grown in 8 well confocal plates (Nunc, Germany) and stimulated according to the experiments performed. Fixation was performed replacing half the media with paraformaldehyde (PFA, 8%), resulting in 4% PFA in the wells. After fixation, the cells were left for 10 min at room temperature. Solution were discarded, and the wells washed with 200 µl PBS and filled with 400 µl PBS, before the plates were wrapped in aluminum foil and stored at 4 °C.

2.6.2 Permeabilization, blocking, staining and imaging

PBS was removed from the wells of the confocal plates. Cold methanol (-20°C, 200 µL, 10 min on ice) was used to permeabilize the cells. Blocking solution (goat serum (3%) and PBS, 200 µL) was added after cells were washed with PBS (200 µL). The confocal plates were left on a shaker at room temperature for 1 h. After 1 h the blocking solution was removed and

primary antibody solution (goat serum (1%), PBS and antibody, 100 µL) was added, and the plates were incubated for 1 h on shaker at room temperature. The primary antibody solution was removed, and the cells were washed with PBS (200 µL, 3x5min). The secondary antibody solution was added (goat serum (1%), PBS, and secondary antibody, 200 µL), and the cells were incubated for 30 min on the shaker at room temperature. The antibody solution was removed and the wells washed with PBS (400 µL, 5x5 min) on shaker. Table 3 and 4 gives a summary of the primary and secondary antibodies, respectively, used in these experiments.

Table 3: Primary antibodies used in immunofluorescence experiments

Antigen	Primary antibody	Manufacture	Dilution
AKT	Mouse monoclonal	Cell signaling	1:200
p-AKT	Rabbit monoclonal	Cell signaling	1:200
m-TOR	Mouse monoclonal	Cell signaling	1:100
p-mTOR	Rabbit monoclonal	Cell signaling	1:50

Table 4: Secondary antibodies used in immunofluorescence experiments

Antigen	Secondary antibody	Manufacture	Dilution
AKT	Alexa Fluor 488goat anti mouse	(Life tech. A11017)	1:5000
p-AKT	Alexa Fluor 555 goat anti rabbit	(Life tech. A11017)	1:5000
m-TOR	Alexa Fluor 488goat anti mouse	(Life tech. A11017)	1:5000
p-mTOR	Alexa Fluor 555 goat anti rabbit	(Life tech. A11017)	1:5000

In the end, PBS was removed and the nuclear staining dye Draq 5 (100 µL, 5µM) was added to each well, and the plates incubated on the shaker at room temperature for 10 min. The solution was removed and the wells were washed with PBS (200 µL, 10 min). The PBS was replaced with 400 µL fresh PBS before wrapping the plates in aluminum foil storing then fridge until microscopy. Subcellular localization was imaged using Axiovert 200 microscope with confocal module LSM 510 Meta with a plan-Apochromat 63x/1.4 oil objective (Carl Zeiss), and analysed using the ZEN 2.3 lite (blue edition).

2.7 Flow Cytometry

2.7.1 Autophagy level measured by Cyto-ID and flow cytometry

DLD-1 and HCT-8 cells were seeded in 6-well plates, while LS411N and LS513 cells were seeded in 12-well plates, respectively. Autophagy level in these cell lines were measured by flow cytometry using the Cyto-ID autophagy detection kit (ENZ-51031-K200, Enzo) that measures the amount of autophagic vacuoles in the cells.

The cells were incubated for 24 h (37 °C, 5% CO_2) before the growth medium was replaced with growth medium supplemented with either EtOH, DHA (70µM), 3-MA (3 mM), Rapamycin (50 nM), DMSO (50 nM) or a combination of two or more of these treatments. Rapamycin is a mTOR inhibitor and autophagy inducer, whereas 3-MA is an autophagy inhibitor. Both treatments were used as control for autophagy level.

After treatment, the cells were incubated for 24 h (37 °C, 5% CO_2) before the medium was discarded and the cells washed with PBS (2 x 1 ml). The cells were detached by trypsination (0.3 ml) for the 12 well plates and 0.75 ml for the 6 well plates) for 8 min. The cells were resuspended in 1,5 ml growth medium, transferred to 15 ml tubes and centrifuged at room temperature, 1000 rpm, for 5 min to get cell pellet. The supernatant was removed, the cell pellet resuspended in 1 ml warm PBS and transferred to Eppendorf tubes before centrifuged once more. The cell pellets were resuspended in 0.25 ml 1x Assay buffer with diluted Cyto-ID detection reagent (0.25 ml). After incubation at 37°C in darkness for 30 min, the cells were centrifuged for 5 min before washed with 1x Assay buffer 0.25 ml. HCT-8 and DLD-1 were then resuspended in 0.35 ml and LS411N and LS513 cells in 0.5 ml 1x Assay buffer, before cells were analysed using flow cytometry (FACSCanto instrument). Data analysis was performed using (FCS Express 6 Plus Research Edition) and Microsoft Excel 2016 software. Fold change between treated and control samples were calculated. Significance was calculated using students t-test (paired, one tailed) and p-values below 0.05 were considered statistically significant.

3. Results

3.1 Four different CRC cell lines respond differently to DHA treatment

In this study, the DHA sensitivity of four different CRC cell lines (LS411N, LS513, DLD-1 and HCT-8) was estimated. The four cell lines were cultivated in the same growth medium and the effect of DHA on growth of the human CRC cell lines was examined by cell counting. The results from cell counting show that DLD-1 and HCT-8 cells are DHA sensitive with a growth inhibition of approximately 45% and 25% for DLD-1 and HCT-8 cells, respectively (fig. 9A). As shown in fig. 9B, the cell growth of LS411N and LS513 cells were almost unaffected by the same treatment, indicating that the growth of these cell lines are almost unaffected by DHA treatment.

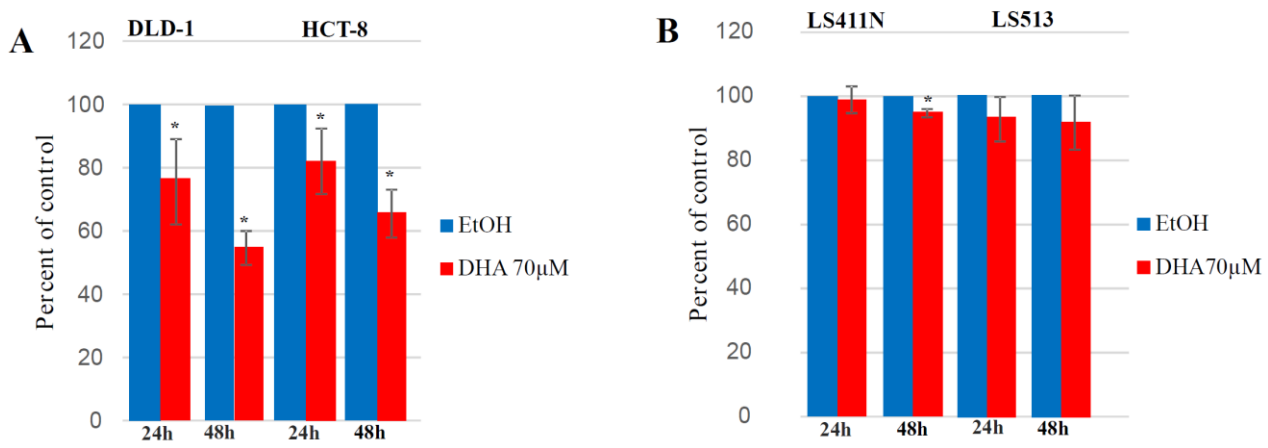

Figure 9: The effect of DHA on cell growth of DLD-1 and HCT-8 cells (A) and LS411N and LS513 cells (B) as measured by cell counting. The cells were treated with 70 µM DHA and counted 24 and 48h after treatment. Control cells were treated with ethanol. The results are presented as mean percent of control and ±standard deviation. The results are based on three or more independent experiments. *Indicates significantly different from control (Student's t-test, paired, on tailed, $p<0.05$).

3.2 Gene expression levels are associated with DHA sensitivity

The gene expression analysis of the four cell lines was investigated. 289 probes were found to be significantly associated with DHA sensitivity (table 5; adjusted p-value <0.05). 153 of these probes were downregulated in DLD-1/HCT-8 cells versus LS411N/LS513 cells, while 146 probes were upregulated in DLD-1/HCT-8 cells versus LS411N/LS513 cells. Some genes were highly differently expressed between the DHA sensitive and less DHA sensitive cell

lines. Some of the genes have known to have an effect on the autophagy process. A positive fold change means that the genes are highly expressed in the DHA sensitive cell lines and vice versa. Inspection of the gene list revealed several differentially expressed probes related to the GO terms ‘’autophagy’’, ‘’lysosome’’, ‘’protein metabolism’’, and ‘’PI3K-AKT pathway’’ (Table 5).

Table 5: Differently expressed genes between DLD-1/HCT-8 cells and LS411N/LS513 cells.

Gene symbol	Probe- ID	Gene title	Log FC	P-value
Autophagy, lysosome, protein metabolism, PI3K-Akt pathway				
AKT3	2126909_s_at	V-akt murine thryoma viral oncogene homolog 3	-0.60	0,03
ANG	205141_at	angiogenin, ribonuclease, RNase A family, 5	-1.68	0,01
AQP3	39248_at	aquaporin 3 (Gill blood group)	-2.79	0.04
ATP1B1	201242_s_at	ATPase, Na+/K+ transporting, beta 1 polypeptide	-2.29	0,01
CAV1	203065_s_at	caveolin 1, caveolae protein, 22kDa	3.29	0,02
CAV1	212097_at	caveolin 1, caveolae protein, 22kDa	4.13	0,02
CBLC	220638_s_at	Cbl proto-oncogene C, E3 ubiquitin protein ligase	-2.62	0,01
CEACAM6	211657_at	carcinoembryonic antigen-related cell adhesion molecule 6 (non-specific cross reacting antigen)	-4.74	0,01
CEACAM6	203757_s_at	carcinoembryonic antigen-related cell adhesion molecule 6 (non-specific cross reacting antigen)	-4.54	0,02
CFTR	215703_at	cystic fibrosis transmembrane conductance regulator (ATP-binding cassette sub-family C, member 7)	-1.95	0,01
CFTR	205043_at	cystic fibrosis transmembrane conductance regulator (ATP-binding cassette sub-family C, member 7)	-3.43	0,01
CREB3L1	213059_at	cAMP responsive element binding protein 3-like 1	-1.49	0,01
CTSH	202295_s_at	cathepsin H	-3.33	0,02
DEPTOR	218858_at	DEP domain containing MTOR-interacting protein	-2.72	0,00
DEPTOR	218858_at	DEP domain containing MTOR-interacting protein	-2.72	0,00
DYRK2	202969_at	dual-specificity tyrosine-(Y)-phosphorylation regulated kinase 2	-1.07	0,04
DYRK2	202968_s_at	dual-specificity tyrosine-(Y)-phosphorylation regulated kinase 2	-1.03	0,03
DPP4	203716_s_at	dipeptidyl-peptidase 4	-2.56	0.04
EEF1A2	204540_at	eukaryotic translation elongation factor 1 alpha 2	2.74	0,03
FGFR2	203638_s_at	fibroblast growth factor receptor 2	-3.06	0,03
FYN	216033_s_at	FYN proto-oncogene, Src family tyrosine kinase	3.09	0,04
GBAP1	210589_s_at	glucosidase, beta, acid pseudogene 1	-1.09	0.04
HIP1	226364_at	huntingtin interacting protein 1	1.86	0,03
HNF4A	230772_at	hepatocyte nuclear factor 4, alpha	-1.16	0,02
KITLG	226534_at	KIT ligand	-3.41	0,03
LYZ	213975_s_at	lysozyme	-6.58	0.00
LYZ	1555745_a_at	lysozyme	-6.50	0.00
MECOM	226420_at	MDS1 and EVI1 complex locus	-4.67	0,00
MECOM	221884_at	MDS1 and EVI1 complex locus	-3.98	0,00
MLEC	200616_s_at	malectin	-1.84	0.04
MUC3B	214898_x_at	mucin 3B, cell surface associated	-1.93	0.03
MUC3B	214676_x_at	mucin 3B, cell surface associated	-1.54	0,02
MUC3A///MUC3	217117_x_at	mucin 3B, cell surface associated	-1.00	0,02
PIGL	205873_at	phosphatidylinositol glycan anchor biosynthesis, class L	1.15	0.04
PIK3R1	212240_s_at	phosphoinositide-3-kinase, regulatory subunit 1 (alpha)	-1.27	0.00
PIK3R1	212239_at	phosphoinositide-3-kinase, regulatory subunit 1 (alpha)	-1.18	0,02
P2RX5	210448_s_at	purinergic receptor P2X, ligand gated ion channel, 5	3.04	0,00
RHOB	1553962_s_at	ras homolog family member B	2.27	0,02
RNASE4	205158_at	ribonuclease, RNase A family, 4	-2.45	0,01
SENP3	203871_at	SUMO1/sentrin/SMT3 specific peptidase 3	0.86	0,02
SMURF2	205596_s_at	SMAD specific E3 ubiquitin protein ligase 2	1.51	0,03
TAB3	227357_at	TGF-beta activated kinase 1/MAP3K7 binding protein 3	0.63	0,03
TMPRSS4	218960_at	transmembrane protease, serine 4	-3.34	0.00

3.3 Differences in the basal level of autophagy in untreated CRC cells

Previous work done in our research group show that the basal level of autophagy might be important for DHA sensitivity in human CRC cell lines. Based on this and the gene expression data, we measured the basal level of autophagy in untreated LS411N, LS513, DLD-1 and HCT-8 cell lines using the Cyto-ID assay and western blot analysis. Cyto-ID

assay produces fluorescence inside the autophagic vesicles. Fluorescence intensity assessed by flow cytometry, showed that the mean fluorescence intensity was higher for the less DHA sensitive LS411N and LS513 cell lines compared to DLD-1 and HCT-8 cells (fig.10). The results from western blot showed a higher basal level of MAP1LC3BII in LS411N and LS513 cells, compared to DLD-1 and HCT-8 cells (fig. 10 B). This indicates a higher basal autophagy level in LS411N and LS513 cells compared to DLD-1 and HCT-8 cells.

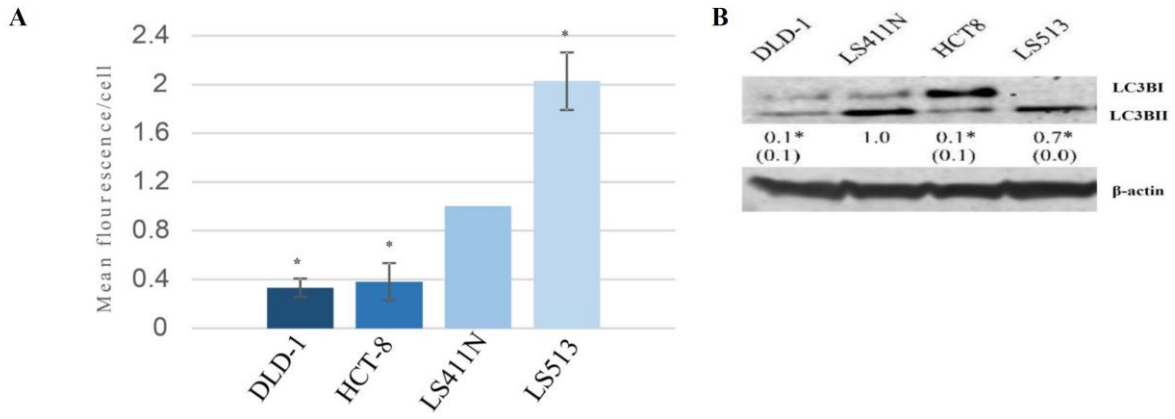

Figure 10: Differences in the basal level of autophagy in untreated LS411N, LS513, DLD-1 and HCT-8 cells, measured by flow cytometry using the fluorescence Cyto-ID assay (A), and by western blotting of MAP1LC3B-II (B). Results represent fold change in mean fluorescence intensity/cell for each cell line, when compared to LS411N cells. *Indicates significantly different from LS411N cells (Student's t-test, paired, one tailed, $p<0.05$).

3.4 DHA sensitivity is associated with the level of autophagy

To determine whether the autophagy level is important for the sensitivity towards DHA, the DHA sensitive cell lines (DLD-1 and HCT-8) were incubated with EtOH, DHA (70µM), DMSO, an autophagy inducer, rapamycin (50nM), or a combination of these. The results from cell counting showed that co-treatment with rapamycin and DHA reduced the DHA-induced growth inhibition about 24% and 15% in DLD-1 and HCT-8 cells, respectively (fig. 11A-D). These results indicate that inducing autophagy may reduce the DHA sensitivity in DLD-1 and

HCT-8 cells.

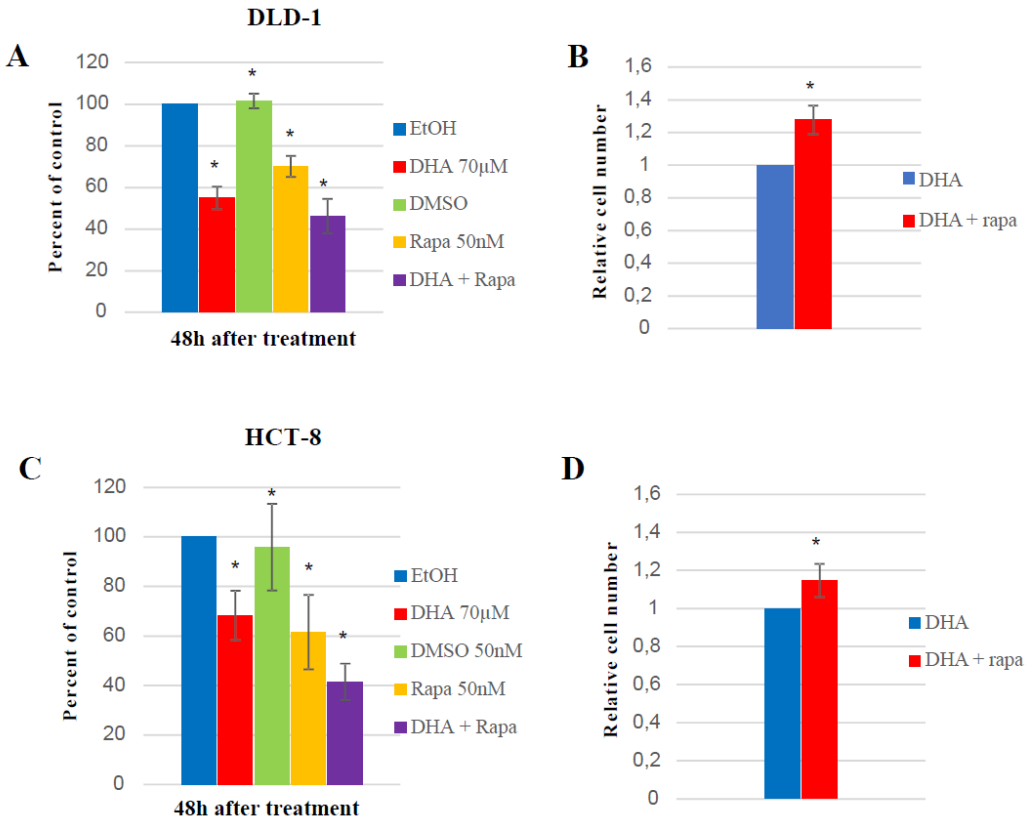

Figure 11: Co- treatment with rapamycin reduces the percent growth-inhibition induced by DHA in DLD-1 and HCT-8. The cells were treated with EtOH, DHA (70 µM), DMSO, rapamycin (50nM) and DHA + rapamycin for 48 h. The results are presented as mean percent of control and standard deviation of DLD-1 (A) and HCT-8 (C) cells and are based on three independent experiments. *Indicates significantly different from control (student's t-test, paired, one tailed $p<0.05$). The results in (B) and (D) are represented as mean relative cell number ± standard deviation after cell counting. Relative cell numbers represent the differences in DHA sensitivity after accounting for the effect of rapamycin alone. *Indicates significant different from DHA treated cells (student's t-test, paired, one tailed $p<0.05$).

The less DHA sensitive cell lines LS411N and LS513 were incubated with EtOH, DHA (70µM) and 3-MA (3mM), which is an autophagy inhibitor, or a combination of these. Co-treatment with 3-MA and DHA increased the growth inhibiting effect of DHA in these two cell lines with approximately 10% and 43% for LS411N and LS513, respectively (fig. 12A and C). Presenting the results as relative cell number, show that the differences in DHA sensitivity are significantly different to the combination treatment with DHA and 3-MA. Compared to DHA treatment (fig. 12B and D), indicating that inhibition of autophagy may increase DHA sensitivity.

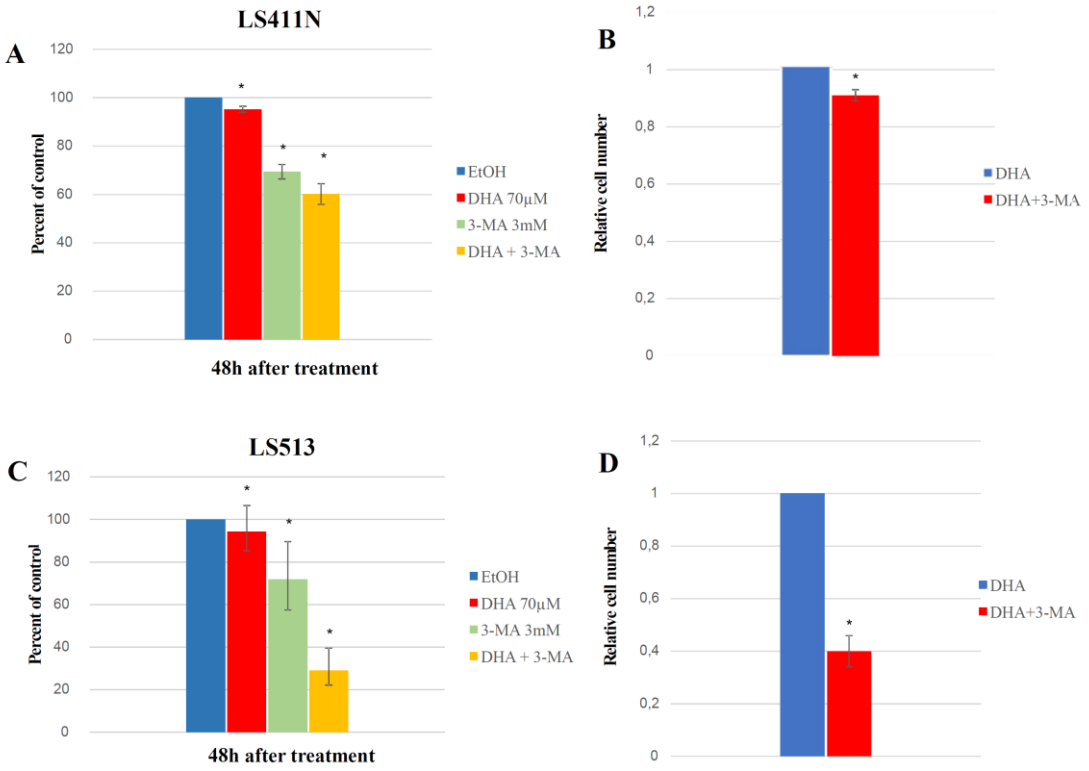

Figure 12: Co- treatment with DHA and 3-MA increases DHA sensitivity in LS411N and LS513 cells. The cells were treated with EtOH, DHA (70 µM), 3-MA (3mM), and 3-MA + DHA. Results are presented as mean percent of control ± standard deviation for LS411N (A) and LS513 (C) cells, and are based on three independent experiments. *Indicates significantly different from control (Student's t-test $p<0.05$). Results in (B) and (D) are represented as relative cell numbers. *Indicates significantly different from DHA treated cells (Student's t-test, paired, one tailed, $p<0.05$).

3.4.1 Microscopic imaging shows that CRC cells respond differently to DHA

The four cell lines included in this study were incubated in the same growth media, and varied in apperance and growth characterisitics. In accordance with the cell counting results (chapter 3.4) the differences in sensitivity toward DHA treatment was also visible in the light microscope. As shown in fig. 13, DLD-1 and HCT-8 cells did not seem to be affected by the control and DMSO treatments, while it was visible that DHA induced growth inhibition in these cells. Rapamycin in combination with DHA reduced the growth inhibition.

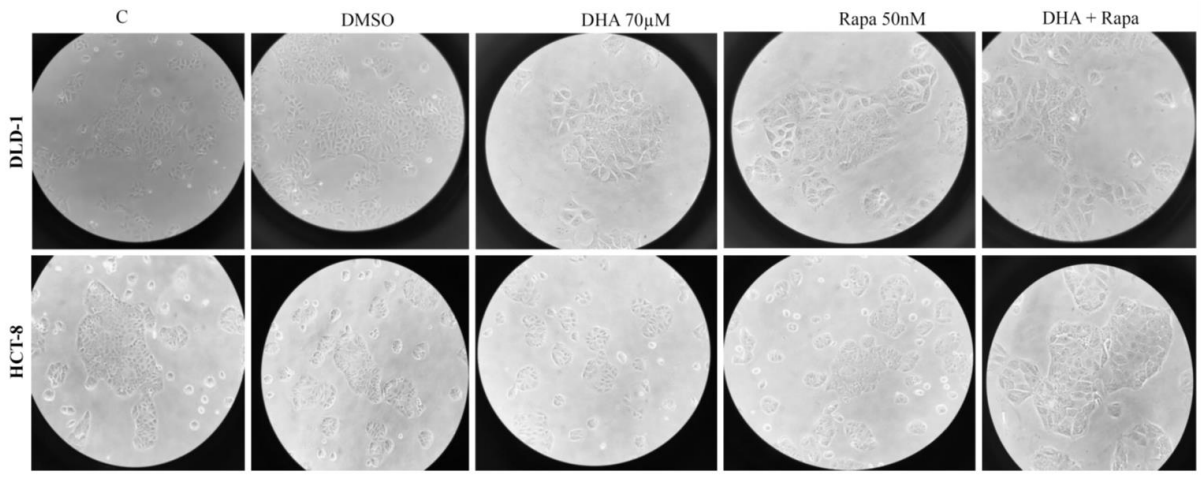

Figure 13: Light microscope images of DLD-1 and HCT-8. The cells were incubated with EtOH (control), DHA, rapamycin and rapamycin + DHA at indicated concentration. Representative images are chosen from three independent experiments.

Images of LS513 and LS411N cells indicated that DHA had no effect on growth of these two cell lines. However, when they were given 3-MA and DHA combined with 3-MA, the cells were clearly growth inhibited as seen in light microscope images (fig. 14), in agreement with the cell counting results.

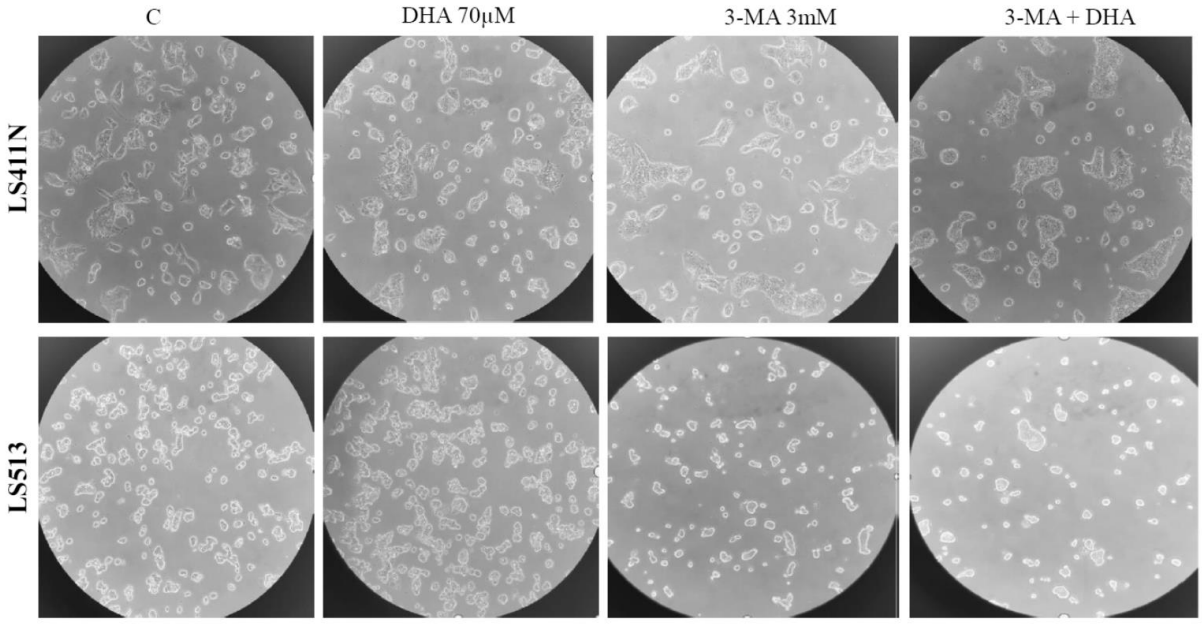

Figure 14: Light microscope images of LS411N and LS513 cells. The cells were incubated with EtOH (control), DHA, 3-MA and 3-MA+DHA, at indicated concentrations. Representative images are chosen from three independent experiments.

3.5 DHA treatment affects autophagy level to different extent in CRC cell lines

To investigate how DHA affects the autophagy level in CRC cells, the level of autophagic vacuoles were assessed using the fluorescent probe Cyto-ID and flow cytometry. The autophagy inducer, rapamycin and the autophagy inhibitor, 3-MA were used alone and in combination with DHA to test how these treatments affected the autophagy level. The results showed that the DHA treatment resulted in a stronger Cyto-ID fluorescence in DLD-1 and HCT-8 cells (fig. 15 A and B). Treatment with rapamycin increased the autophagy level, and in combination with DHA to an even higher level than rapamycin alone. For the less DHA sensitive cell lines LS411N and LS513 (fig.15 C and D), the DHA treatment seemed to decrease autophagy levels compared to control. When treated with 3-MA, a decrease of Cyto-ID fluorescence intensity was measured, indicative of a reduction in the level of autophagic vacuoles level, and therefore a decrease of Cyto-ID fluorescence intensity was measured. The co-treatment with 3-MA and DHA led to a decrease in autophagy level, compared to 3-MA alone.

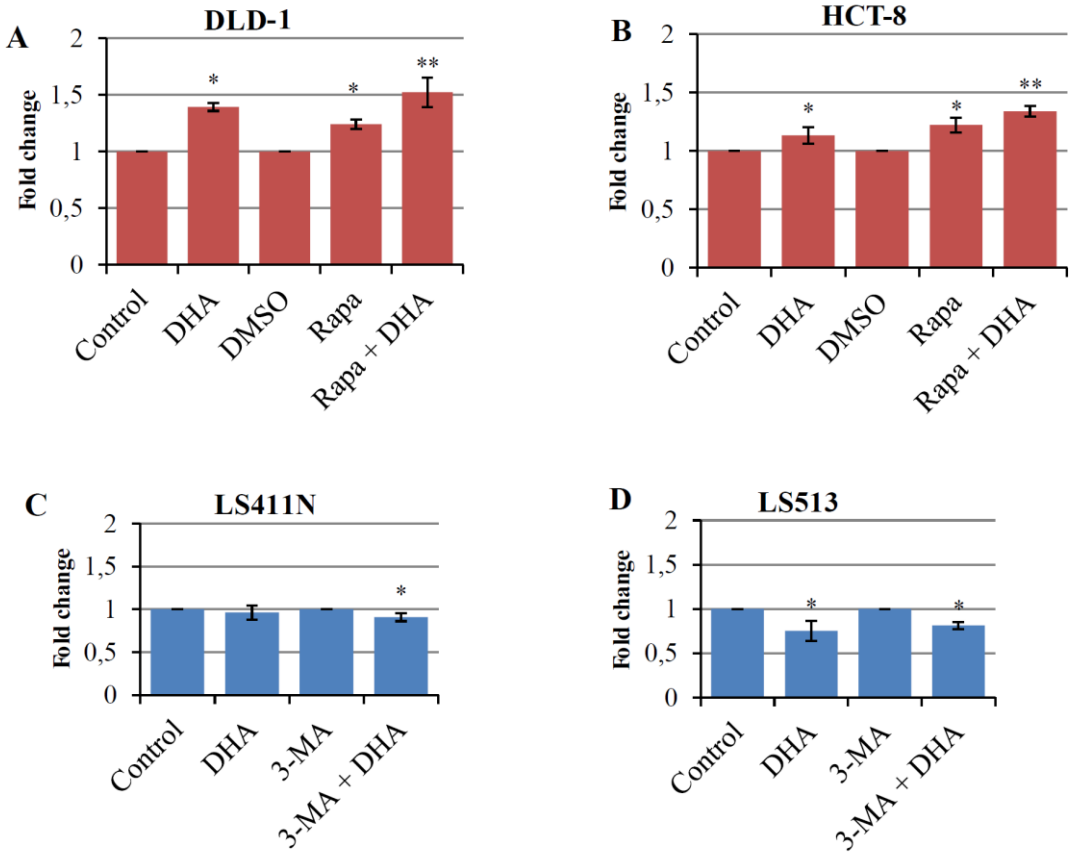

Figure 15: The level of autophagy measured by the fluorescent probe Cyto-ID and flow cytometry in DLD-1 (A), HCT-8 (B), LS411N (C) and LS513 cells (D). DLD-1 and HCT-8 cells were treated with EtOH (control), DHA (70µM), DMSO (50 nM), rapamycin (50 nm) and co-treatment with DHA (70 µM) and rapamycin (50 nm) for 24h. LS411N and LS513 cells were treated with EtOH (control), DHA (70 µM), 3-MA (3 mM), and DHA (70 µM) in combination with 3-MA (3 mM) for 24h. The results are based on three independent experiments ± standard deviation. The results are presented as fold change (fluorescence/cell) compared to respective controls (EtOH, DMSO or 3-MA). *Indicates significantly different from its controls. **Indicates significantly different from control and DHA treatment (student's t-test, paired, one tailed, $p<0.05$).

Autophagy levels measured by the Cyto ID assay, may also be presented as fluorescence intensity per cell (fig. 16 and 17). The DHA sensitive DLD-1 and HCT-8 cells were treated with EtOH (control), DHA (70 µM), DMSO, rapamycin (50 nM) or a combination of these. Results presented in fig. 16 show that DHA- treated DLD-1 and HCT-8 cells are more intensively stained compared to control cells. Rapamycin treatment increased the level of stained autophagic vacuoles, and to an even higher level when co-treated with DHA.

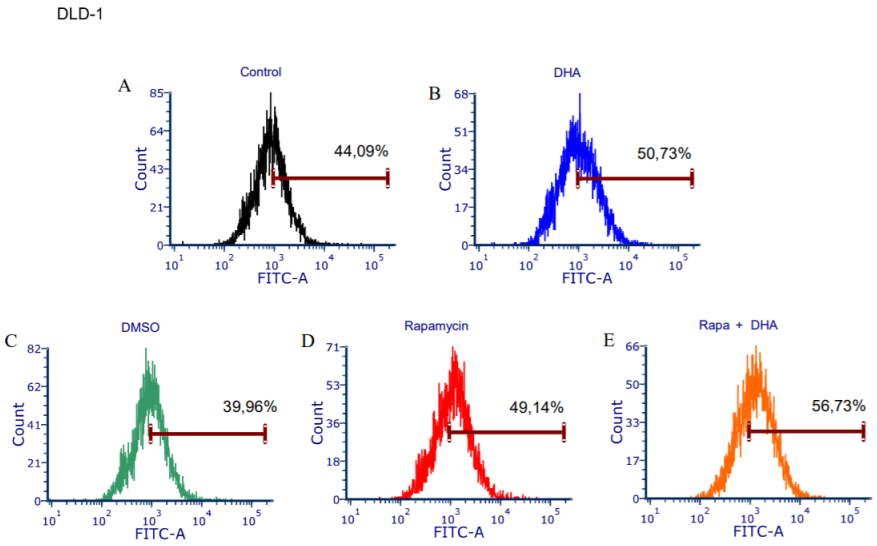

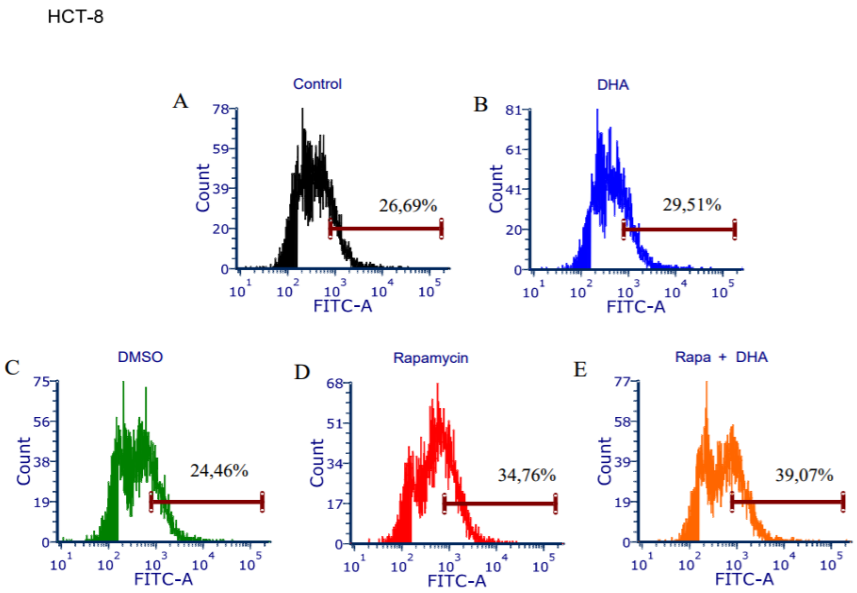

Figure 16: Flow cytometry and fluorescent probe Cyto-ID analysis for DLD-1 and HCT-8 cells treated with EtOH (control), DHA (70µM), DMSO, Rapamycin (50nM), and DHA+ rapamycin. The percent represent show cells that have fluorescence level within the gated area, and is based on three independent experiments. X-axis represent level of fluorescein isothiocyanate (FITCA) staining. Y-axis represent cell count (10 000 cells were counted for each sample). One representative diagram for each treatment is shown.

LS411N and LS513 were incubated with EtOH, DHA (70 µM), 3-MA (3 mM) and a combination of DHA and 3-MA. The results presented in fig. 17 show that the DHA treatment of LS411N and LS513 cells gave a higher number of cells with low fluorescence intensity. This indicate that DHA and DHA in combination with 3-MA reduced the staining of autophagic vacuoles in these cell lines, and thereby the autophagy level.

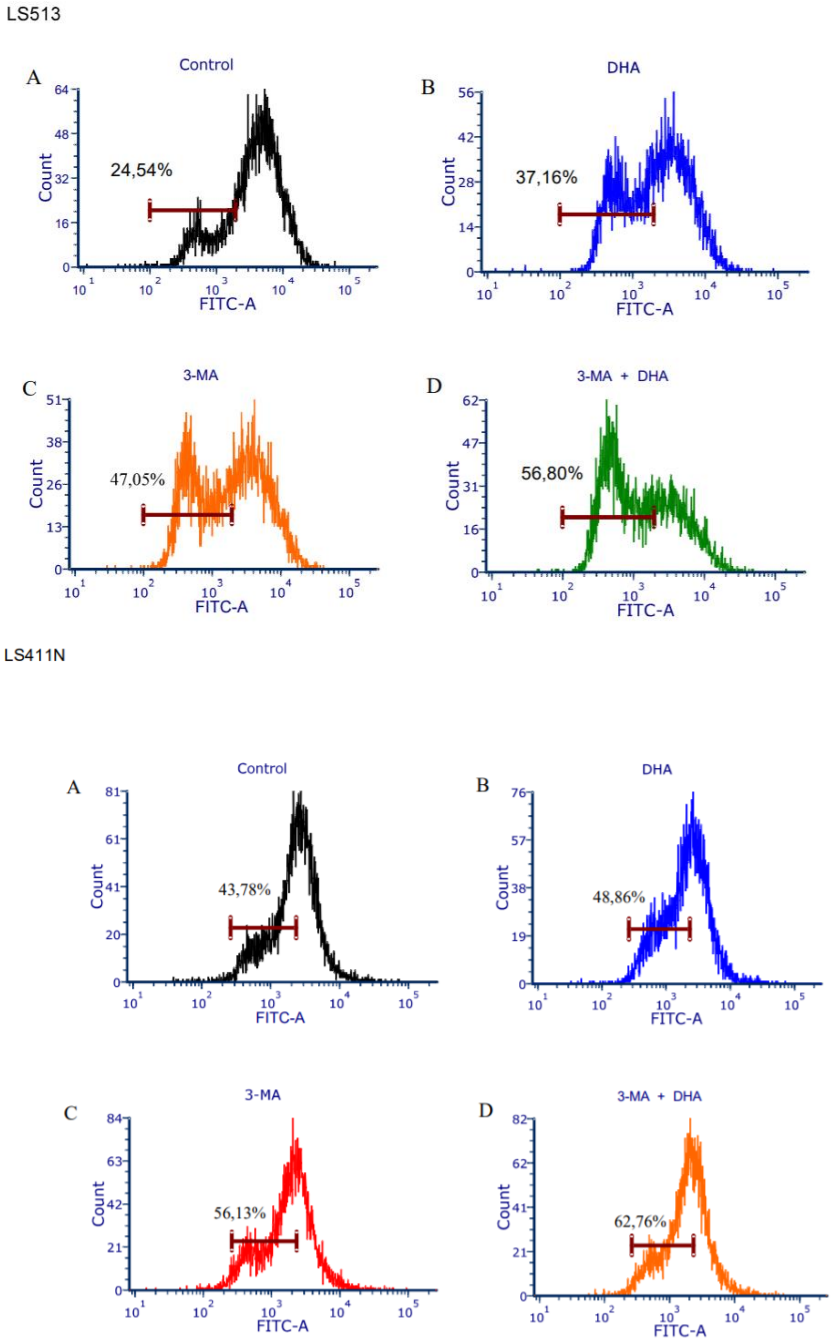

Figure 17: Flow cytometry and fluorescent probe Cyto-ID analysis for LS411N and LS513 cells. Cells treated with EtOH (control), DHA 70µM), 3-MA (3mM) and DHA + 3-MA. The percent presents cells (10 000 cells counted for each sample) with fluorescence level within the gated area with different treatments, based on three independent experiments. One representative diagram for each treatment is shown.

3.6 DHA increased the level of the autophagy marker protein MAP1LC3BII in DHA sensitive CRC cells

MAP1LC3B-II is the most well-characterized protein that is localized to autophagic structures through the process from phagophore to lysosomal degradation [44]. To detect whether differences between the four cell lines in the ability to induce autophagy could explain the difference in DHA sensitivity, the levels of the MAP1LC3B-II protein was measured by western blot analysis. The DHA sensitive cell lines, DLD-1 and HCT-8, were incubated with EtOH, DMSO, DHA (70 µM), rapamycin (50 nM) or a combination of these. The results show that the protein level of MAP1LC3B-II increased by DHA treatment after 24h in these two cell lines compared to the control cells. We observed that the amount of MAP1LC3B-II was also increased by rapamycin, and to an even higher level with a combination treatment with DHA and rapamycin (fig. 18A). The less DHA sensitive LS513 and LS411N cells were incubated with DHA (70 µM), the autophagy inhibitor 3-MA (3 mM), or a combination of these. The results indicated that DHA treatment reduced the level of MAP1LC3B-II in these cells. 3-MA gave a higher level of MAP1LC3BII, however this level decreased with co-treatment with DHA and 3-MA (fig. 18B). These findings indicate that the autophagic flux is increased by DHA for the DHA sensitive cell lines, while autophagic flux are decreased by DHA in less DHA sensitive cell lines.

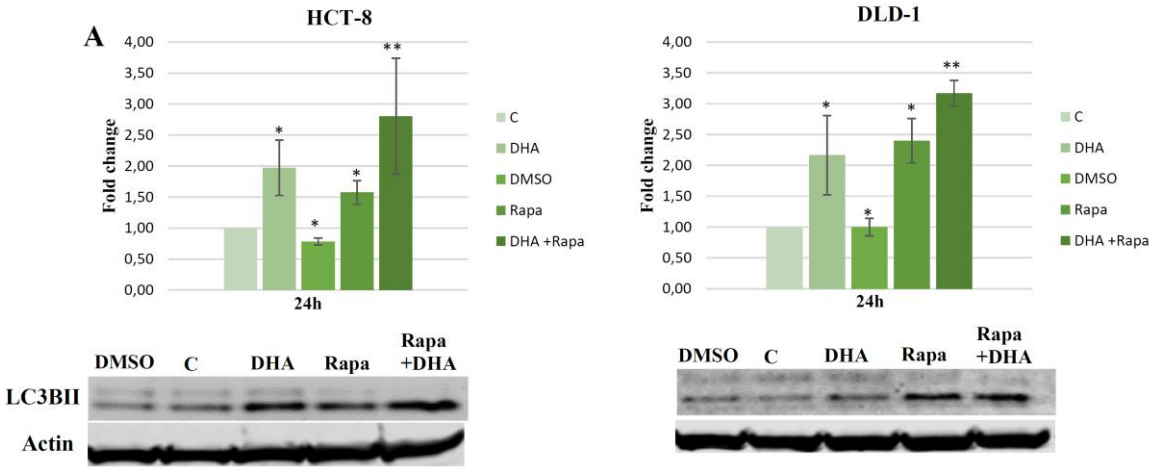

Figure 18 A: Protein expression level of MAP1LC3BII in DLD-1 and HCT-8 cells (A). The cells were incubated in EtOH (C), DHA (70 µM), rapamycin (50 mM), or a combination of rapamycin and DHA. The results represent fold change for band intensities of MAP1LC3BII compared to control, based on three independent experiments. The band intensities are normalized against β-actin. *Indicates significantly different from control cells (Student's t-test, paired, one tailed, ($p<0.05$). ** Indicates significantly differently from rapamycin treated cells, and 3-MA treated cells (Student's t-test, paired, one tailed $p<0.05$).

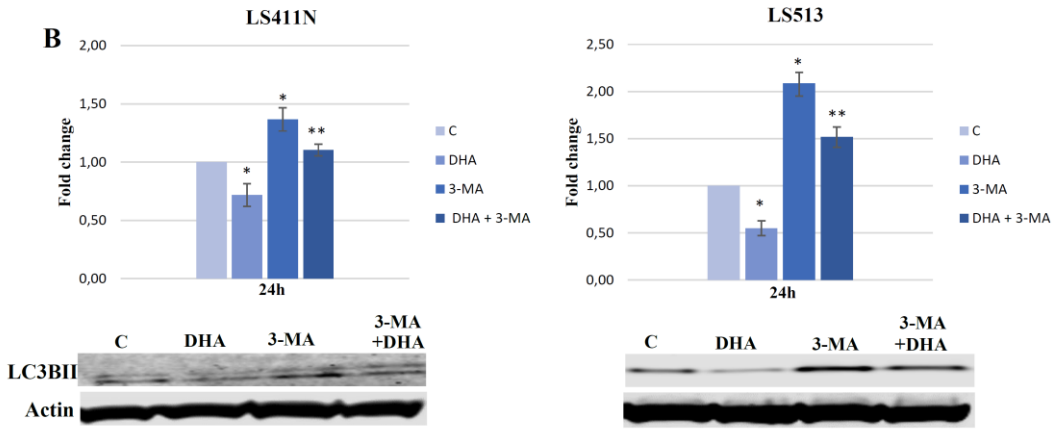

Figure18 B: Protein expression level of MAP1LC3BII in LS411N and LS513 cells (B). The cells were incubated in EtOH (C), DHA (70 µM), 3-MA (3mM) or a combination of these treatments. The results represent fold change for band intensities of MAP1LC3BII compared to control, based on three independent experiments. The band intensities are normalized against β-actin. *Indicates significantly different from control cells (Student's t-test, paired, one-tailed, $p<0.05$). ** Indicates significantly differently from rapamycin treated cells, and 3-MA treated cells (Student's t-test, paired, one tailed $p<0.05$).

3.7 DHA affects AKT signaling in both DHA sensitive and less DHA sensitive CRC cell lines

The PI3K/AKT pathway plays a crucial role in CRC development, and inhibition of this signaling pathway may activate autophagy in cancer cells. Phosphorylated AKT (p-AKT) activates mTOR, which leads to negative regulation of autophagy [49, 50]. We hypothesized that AKT signaling inactivation might be involved in the induction of autophagy during DHA treatment in the DHA sensitive CRC cell lines. To test this, we first examined the effect of EtOH (control) and DHA on AKT and phosphorylated AKT expression by western blotting. The p-AKT level of the four CRC cell lines had a tendency to increase at early time points of DHA incubation. After 24 h, DHA led to a slightly decrease in phosphorylated AKT levels in both DHA sensitive and less DHA sensitive cell lines compared to control (fig. 19 and 20A and B). The changes in protein level of total AKT seems to have the same trend as p-AKT for the four cell lines (fig. 19 and 20 C and D).

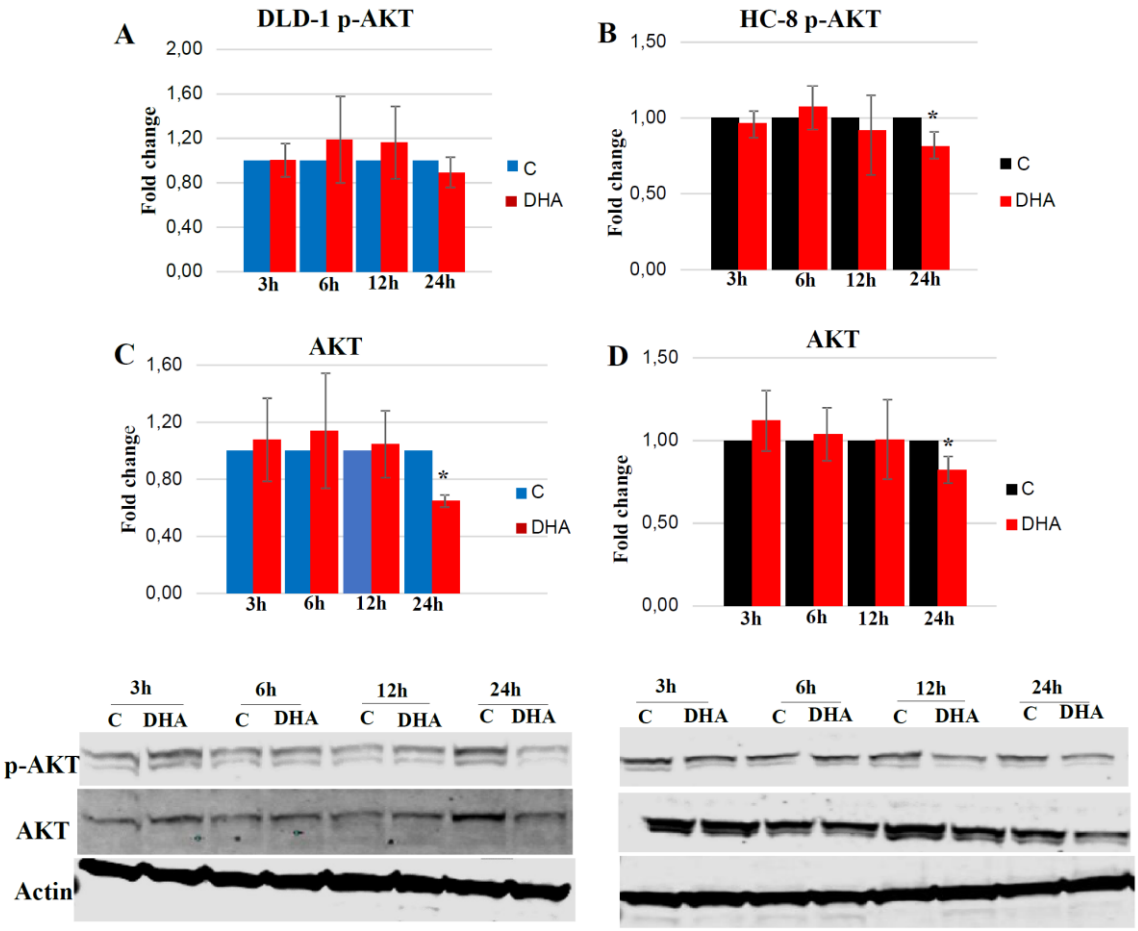

Figure 19: Protein expression level of p-AKT and AKT at different time points in DLD-1 cells (A and C) and HCT-8 cells (B and D), treated with EtOH (C) and DHA (70 µM). The fold change value of these proteins is correlated to β-actin. The results are based on three independent experiments. *Indicates significantly different from control (Student's t-test, paired, one tailed $p<0.05$).

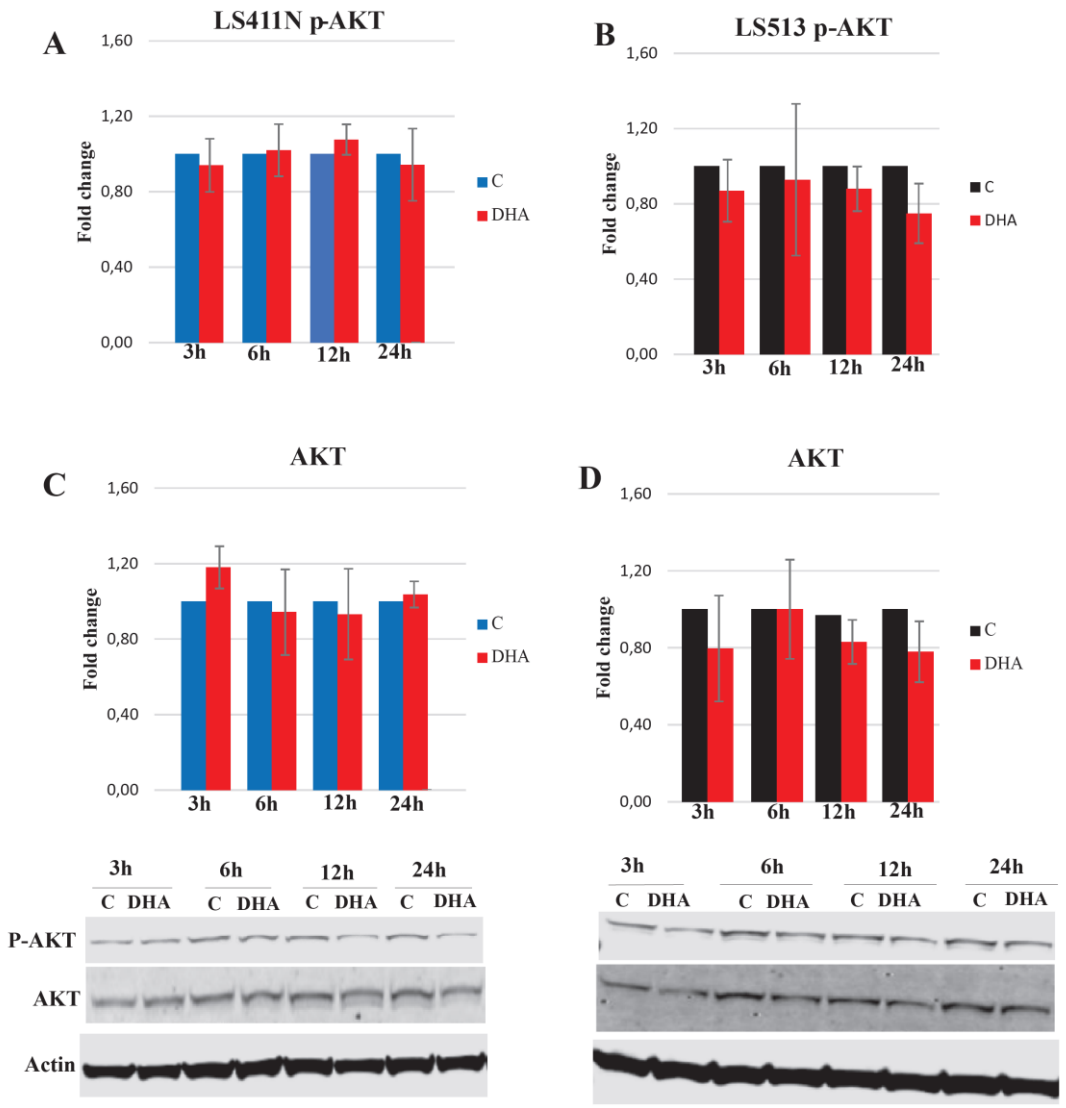

Figure 20: The protein expression level of p-AKT and total AKT at different timepoints in the LS411N (A and C) LS513 cells (B and D), treated with EtOH (C) and DHA (70 µM). The band intensities are normalized against the loading control β-actin. The results are based on three independent experiments.

To further investigate the DHA on p-AKT and AKT levels, DLD-1 and HCT-8 cells were treated with EtOH (control), DHA (70µM), DMSO, rapamycin (50nM) or combination of these treatment. After 24 h treatment, results showed that both DHA and rapamycin alone decreased the level of p-AKT significantly compared to control in DLD-1 and HCT-8 cells. Co-treatment with DHA and rapamycin further decreased the p-AKT level compared to rapamycin alone (fig.21 A and B). The total AKT level also seemed to decrease for these cell lines but not as much as p-AKT (fig. 21 C and D).

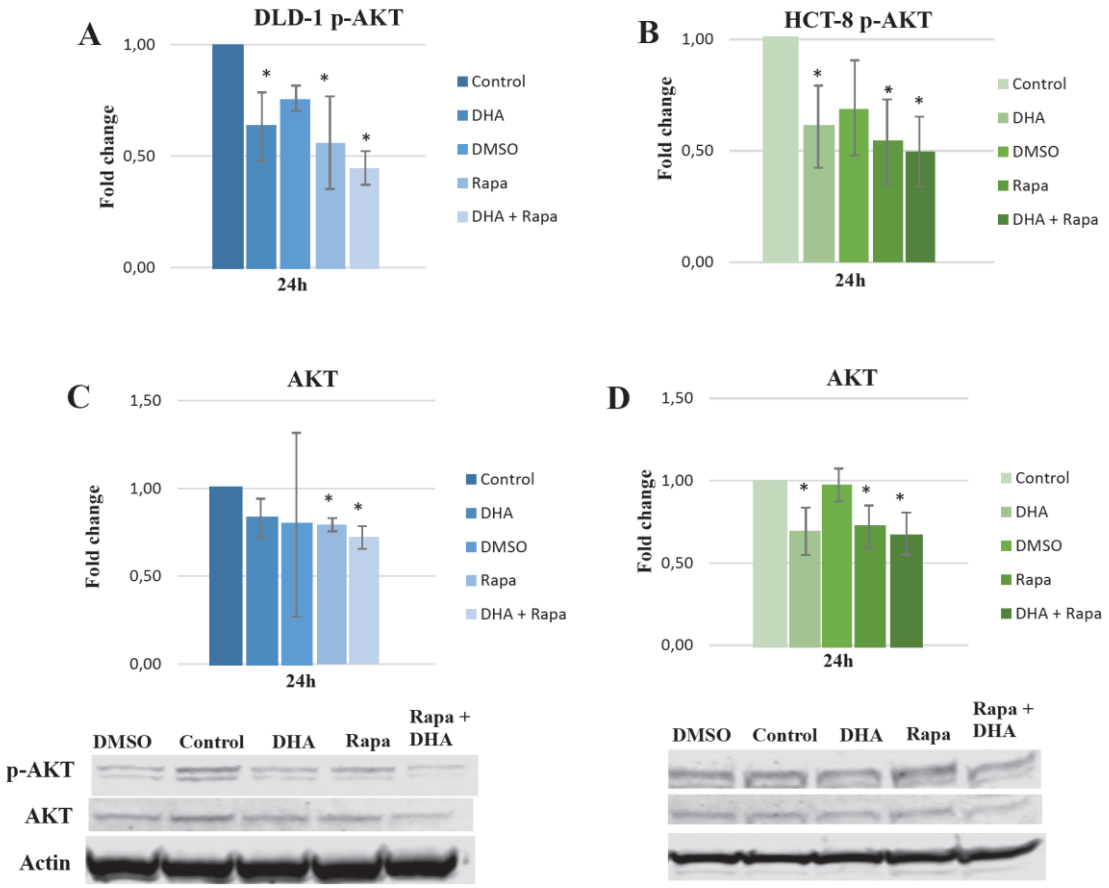

Figure 21: The protein expression level of p-AKT (A and B) and total AKT (C and D) in DLD-1 and HCT-8 cell, respectively. The cells were treated with EtOH (control), DHA (70 µM), DMSO (50 nM), rapamycin (50 nM) or combination of these. The fold change values of total and p-AKT are normalized to loading control (β-actin). The results are based on three independent experiments. *Indicates significantly different from control (Student's t-test, paired, one- tailed, $p<0.05$).

The less DHA sensitive cell lines (LS411N and LS513) were incubated with EtOH (control), DHA (70µM), 3-MA (3mM) alone or combination with DHA. We observed that DHA reduced p-AKT slightly compared to control in LS513 but not in LS411N. The autophagy inhibitor, 3-MA seemed to increase the level of p-AKT, while co-treatment with DHA and 3-MA tended to decrease the p-AKT level (fig. 22). Total AKT seemed to have the same trend as p-AKT also for these cell lines but not to the same extents.

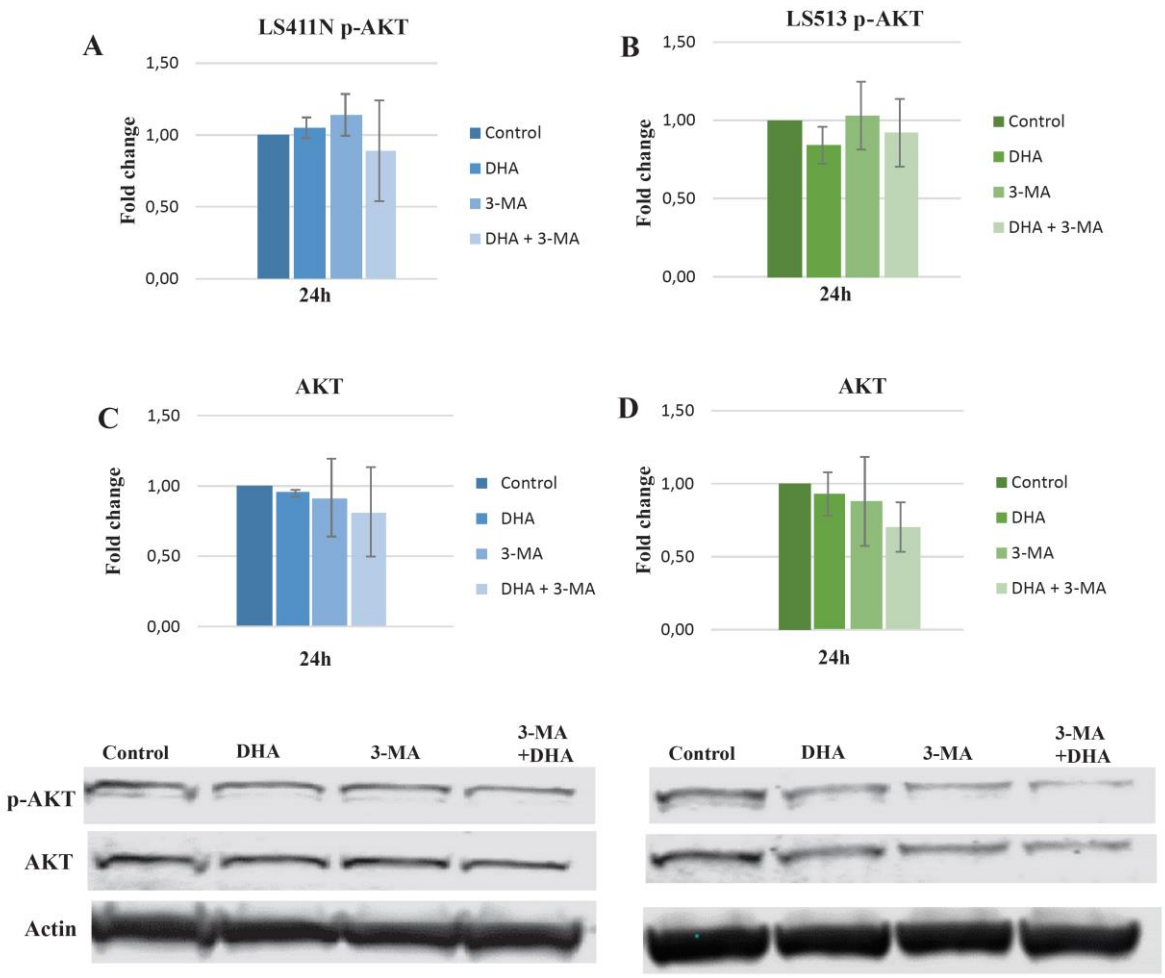

Figure 22: The protein expression level of p-AKT (A and B) and total AKT (C and D) in LS411N and LS513, respectively. The cells were treated with EtOH (control), DHA (70 µM), 3-MA (3 mM), or a combination of these. The fold change values of p-AKT and AKT are normalized to loading control (β-actin). The results are based on three independent experiments. *Indicates significantly different from its control. (Student's t-test, paired, one- tailed, $p<0.05$)

3.8 Confocal imaging indicates differences in the effect of DHA on p-AKT protein expression

To obtain more information on the p-AKT and total AKT levels in these four cell lines, confocal imaging of DLD-1 and HCT-8 cells immunostained for AKT and p-AKT was performed 24 h after treatment with EtOH (C), DHA (70 µM), DMSO, and rapamycin (50 nM), or a combination of these, to examine levels and cellular localization of the proteins. The results show that the cells stained for total AKT (green) were almost unchanged in both cell lines. Confocal imaging indicated that p-AKT is localized in the nucleus in DLD-1 and HCT-8 control cells (fig. 23 A and B). DHA treatment of these cell lines seemed to reduce the

positive nuclear staining and total level of p-AKT (fig. 23 A and B). Treatment with the autophagy inducer, rapamycin and rapamycin together with DHA seemed to reduce the positive nuclear staining of p-AKT even more for these two cell lines.

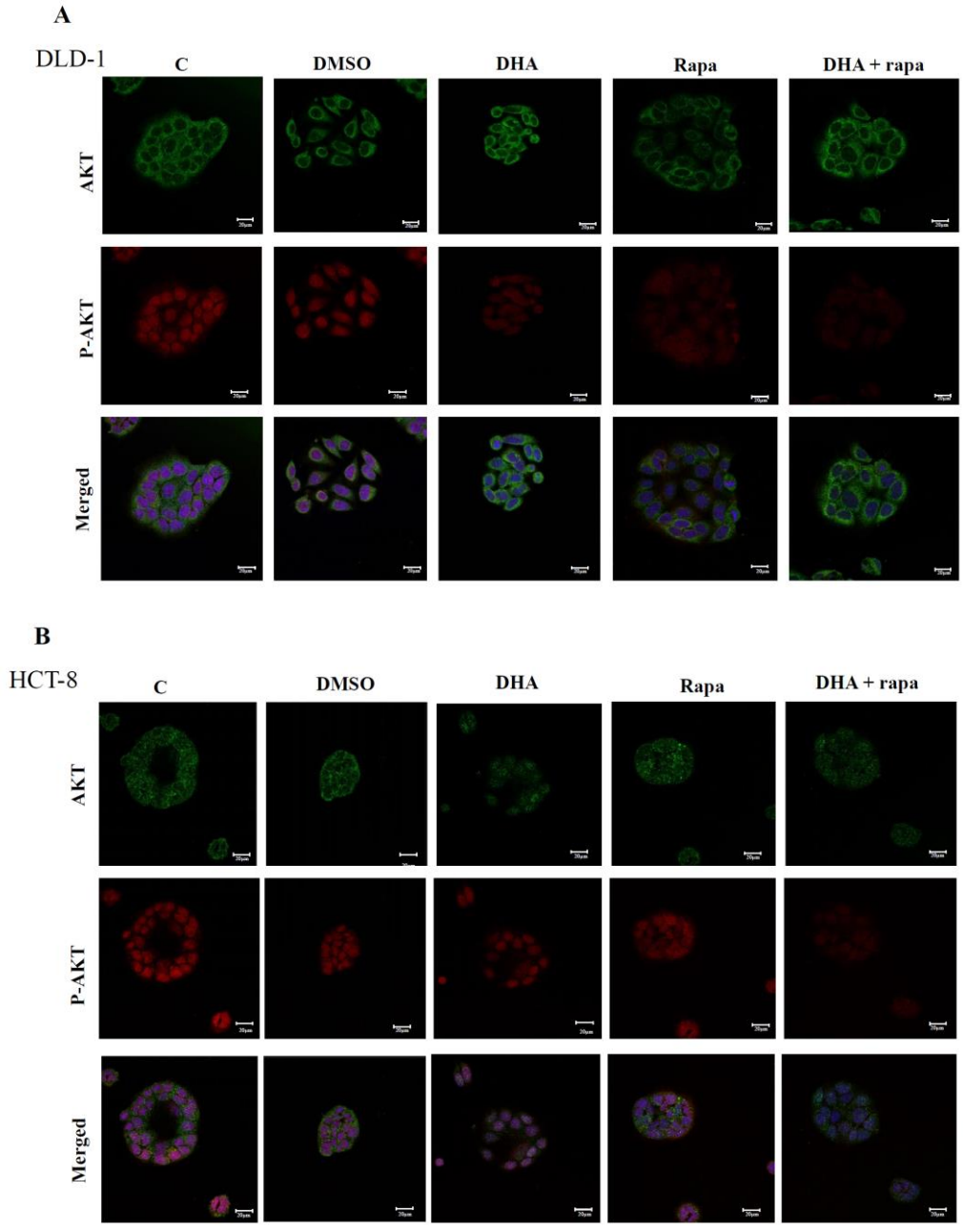

Figure 23: Cellular localization and protein level of AKT and P-AKT in DLD-1(A) and HCT-8 (B) cells 24h after treatment with EtOH (C), DHA(70µM), Rapamycin (50 nM), or a combination of these treatments, shown by confocal images of cell immunostained with AKT (green) and p-AKT (red). Draq5 (nuclear) is stained in blue. Result are based on three independent experiments. One representative image per treatment is shown. Scale bar 20 µm.

For LS411N and LS513 cells, the class III PI3K inhibitor 3-MA were used to block autophagy activation. Inhibition of PI3K leads to inhibition of autophagosomes formation and the autophagic process eventually fails [62, 63]. Both DHA (70 µM) and 3-MA (3mM) treatment increased the level of p-AKT and the co-treatment even more (fig. 24 A and B).

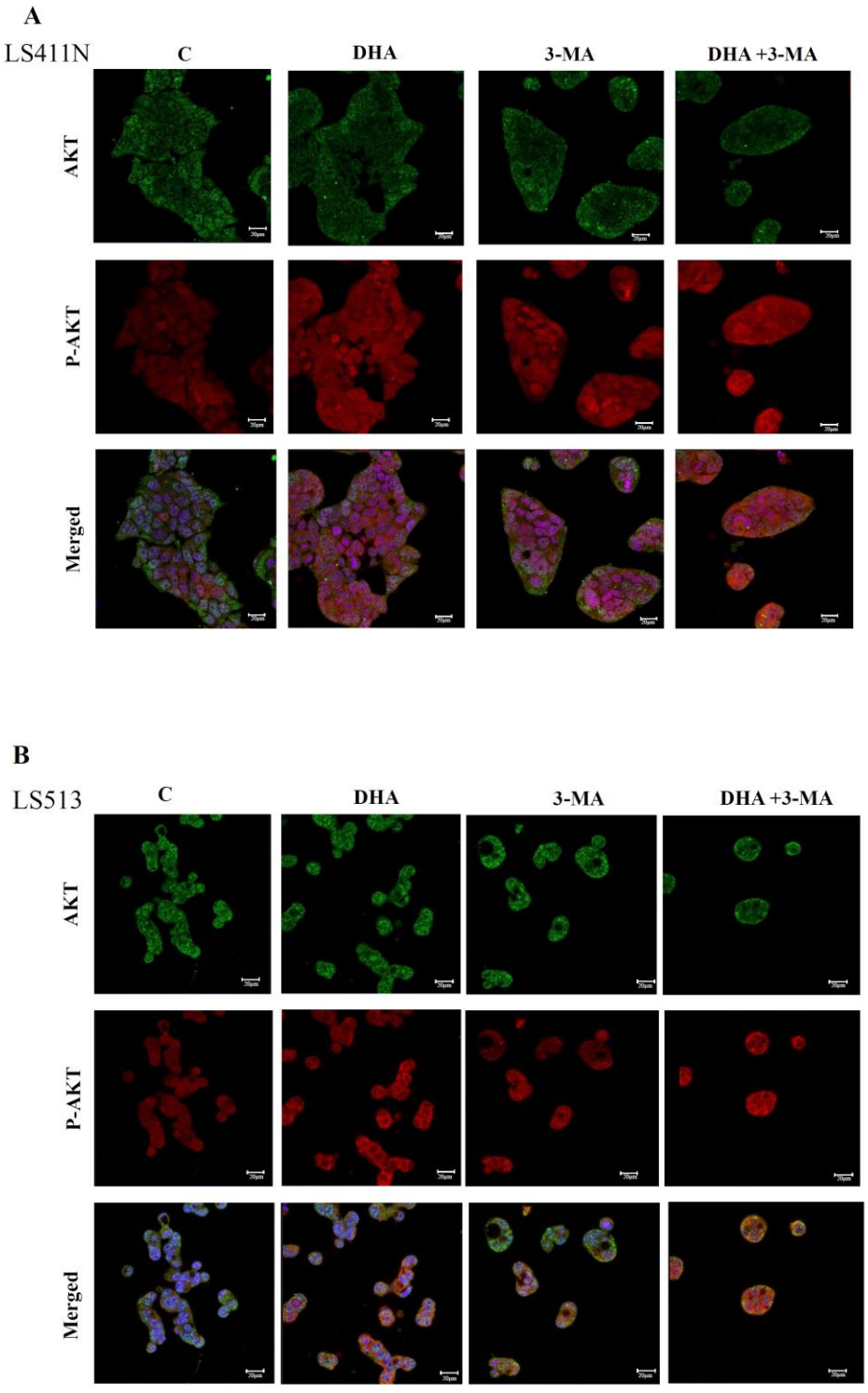

Figure 24: Cellular localization and protein level of AKT and P-AKT in LS411N (A) and LS513 (B) cells 24h after treatment with EtOH (C), DHA(70µM), 3-MA (3mM), or a combination of these treatments, shown by confocal imaging of cell immunostained with AKT (green) and p-AKT (red). Nuclear Draq5 is stained in blue. Results are based on three independent experiments. One representative image per treatments is shown. Scale bar 20 µm

3.9 DHA treatment has different effect on p-mTOR expression in DHA sensitive and less DHA sensitive CRC cells

The mTOR pathway is a key regulator of cell growth and proliferation and is involved in many diseases, including CRC. m-TOR is activated by AKT and it is a negative regulator of autophagy. Thus, we wanted to examine whether the protein level of mTOR is affected by DHA. The protein level of m-TOR and p-mTOR, were investigated in the four CRC cell lines after treatment with EtOH (C), DHA (70 µM), DMSO, rapamycin (50 nM) and DHA combined with rapamycin in DLD-1 and HCT-8 cells. Results show that DHA and rapamycin, both alone and in combination, reduced the levels of p-mTOR in the DHA sensitive cell lines (DLD-1 and HCT-8 cells). Total mTOR seemed to have the same trend as p-mTOR for both cell lines. However, some of the band were almost not visible.

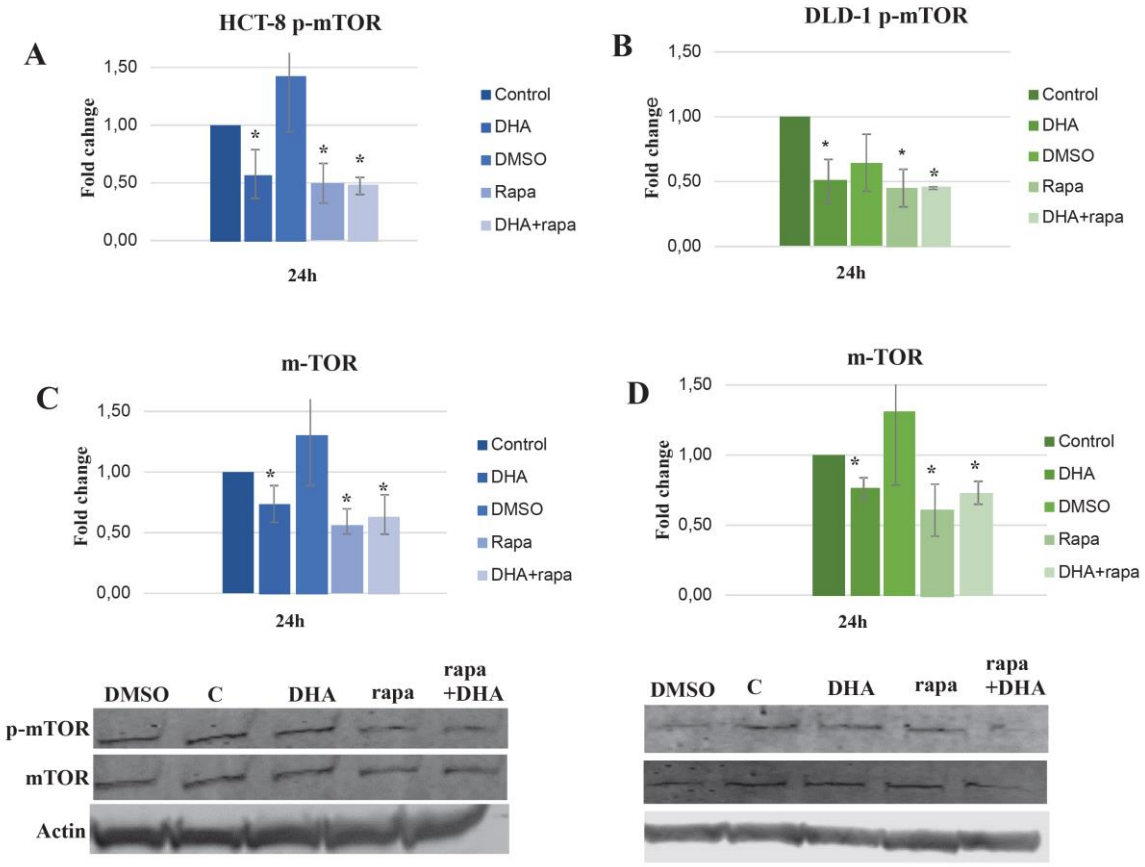

Figure 25: Western blot of the p-mTOR and mTOR proteins in DLD-1 and HCT-8 cells. Cells were incubated with the EtOH (C), DHA (70 µM), rapamycin (50 nM) and a combination of rapamycin and DHA for 24 h. Band intensities are normalized against loading control β-actin. Results are presented as mean fold change of three independent experiments. *Indicates significantly different from control. (Student's t-test, paired, one- tailed, $p<0.05$)

The less DHA sensitive cell lines LS41N and LS513, were incubated in EtOH (C), DHA (70 µM), 3MA (3 mM) and 3-MA combined with DHA. The results from western blot indicated an increase in the p-mTOR level after DHA treatment in these cells (fig. 26A and B). The total protein level of mTOR seemed to have the same trend as p-mTOR in both cell lines (fig. 26 C and D).

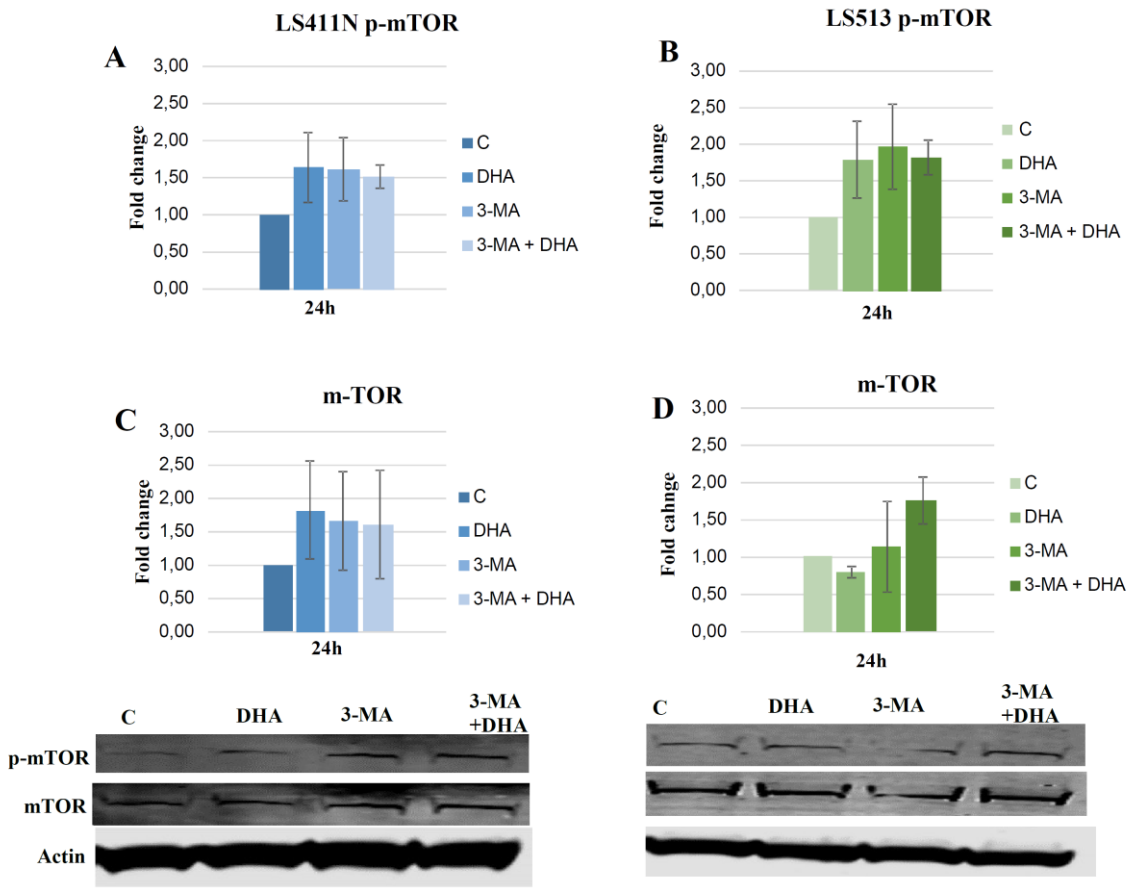

Figure 26: Protein expression levels of p-mTOR (A and B) and mTOR (C and D) for LS411N and LS513 cells, respectively. The cells are treated with EtOH (C), DHA (70 µM), 3-MA (3 mM) and DHA combined with 3-MA for 24 h and then subjected to western blot analysis with antibody against p-mTOR, mTOR and β-actin. Band intensities are normalized against the loading control (β-actin). Results are presented as mean fold change based on three independent experiments. One representative band is shown. *Indicates significantly different form control.

To further examine the effect of DHA treatment on mTOR expression, the level of p-mTOR and total mTOR was investigated using confocal imaging. The results indicate that the level of p-mTOR seems to decrease with DHA treatment compared to control for both DLD-1 and HCT-8 cells (fig. 27A and B). The level of total m-TOR was almost unchanged for both cell lines (fig. 27 A and B). These results indicate that DHA inhibits the mTOR pathway.

The level of p-mTOR in LS411N and LS513 was increased compared to control after DHA treatment for 24h (fig. 28 A and B), while the total mTOR seemed to be unchanged.

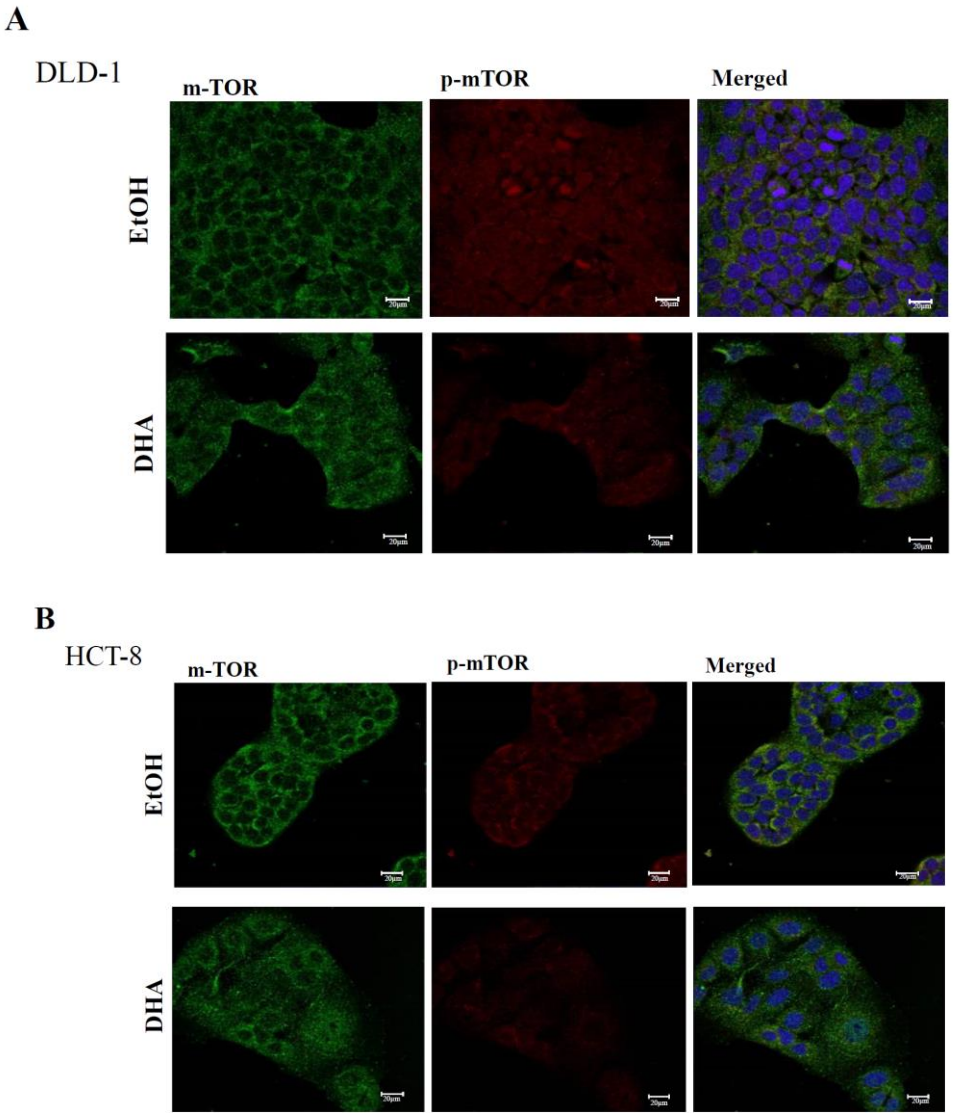

Figure 27: Cellular localization and protein level of p-mTOR and total mTOR in DLD-1 cells (A), HCT-8 cells (B), after treatment with EtOH, DHA (70 µM), DMSO, Rapamycin (50 nM) or a combination of these for 24 h, shown by confocal images of cell immunostained with mTOR (green) and p-mTOR (red). Draq5 (nuclear) stained blue. Results are based on three independent experiments. One representative image is shown for each treatment. Scale bar 20 µm.

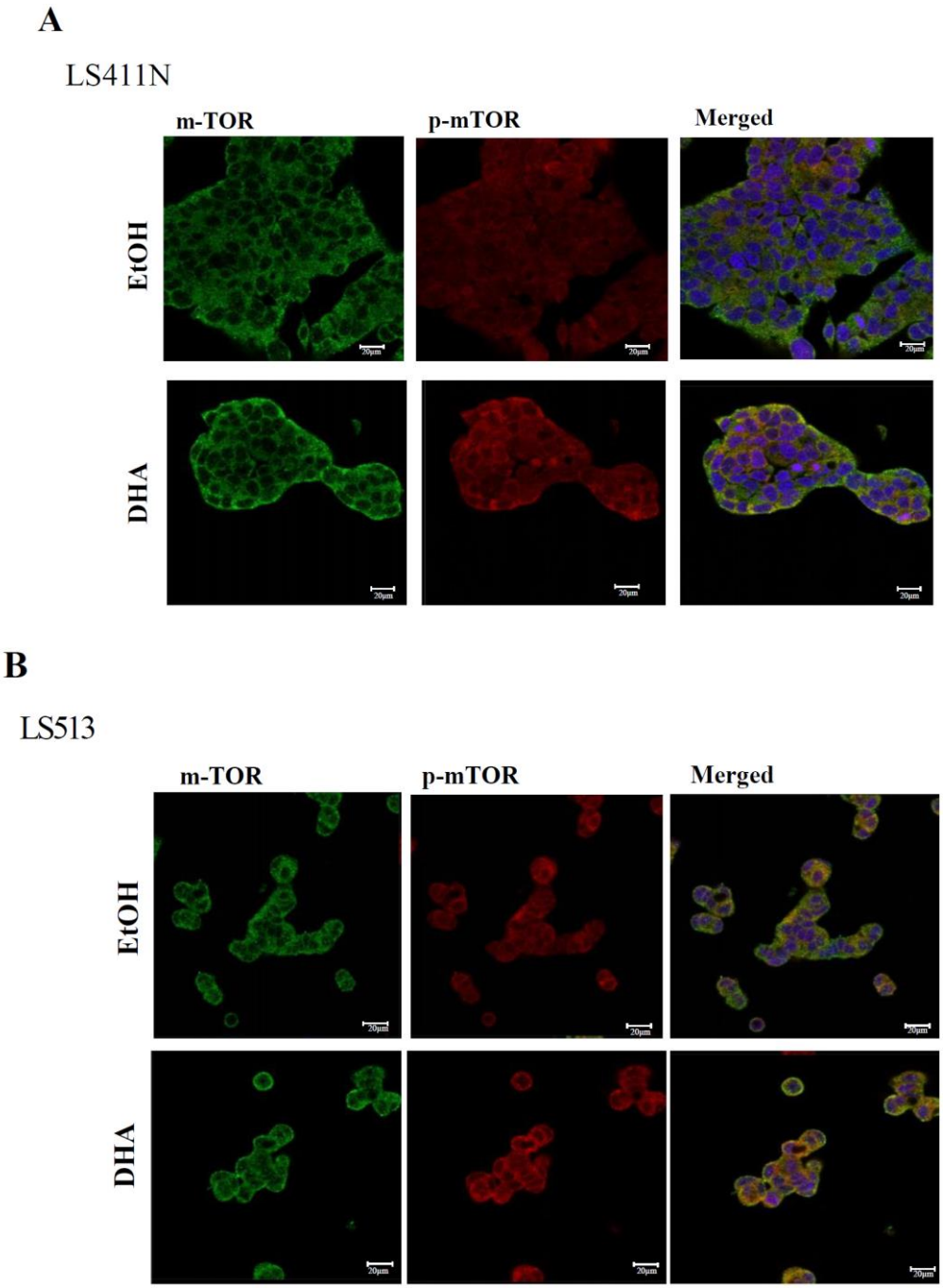

Figure 28: Cellular localization and protein level of p-mTOR and total mTOR in LS411N cells (A) and LS513 cells (B) after treatment with EtOH, DHA (70 µM), DMSO, 3-MA (3 mM), rapamycin (50 nM) or a combination of these for 24 h, shown by confocal images of cell immunostained with mTOR (green) and p-mTOR (red). Draq5 (nuclear) in blue. Results are based on three independent experiments. One representative image is shown for each treatment. Scale bar 20 µm.

4. Discussion

Several studies have established that some n-3 PUFAs have a potential for prevention and therapy of several types of cancer, including CRC. Different cancer cell lines are known to respond differently to DHA treatment. The results presented in this thesis show that the CRC cell lines DLD-1, HCT-8, LS411N, and LS513 respond differentially to treatment with a physiologically relevant dose of DHA (70 µM). HCT-8 and DLD-1 cell lines are sensitive to DHA treatment and have a low basal level of autophagy, which increased after treatment with DHA (70 µM). Oppositely, LS411N and LS513 cells are less DHA sensitive and have a higher level of basal autophagy, which decreased after DHA (70 µM) treatment.

4.1 DHA induced different growth response in four human CRC cell lines

DHA sensitivity was estimated by cell counting in four CRC cell lines. The data presented here clearly shows that the DLD-1 and HCT-8 cell lines are sensitive to DHA, with a growth inhibitory effect of ~25-45 % after 48 h. LS411N and LS513 cells responded less to DHA treatment, indicating that these cell lines are less DHA sensitive. These results correlate with previous and recently findings by our group, which showed that CRC cell lines responded differently to DHA treatment [1, 36].

The studied cell lines were incubated in the same growth medium, to avoid possible influences from differences in media components. Previous studies have shown that differences in serum concentration in the growth medium may affect DHA sensitivity between cancer cells [64]. Findings from several groups have shown that serum seems to have a protective effect, meaning that cell lines with higher serum concentrations in the medium tolerate treatment with n-3 PUFAs better [65]. Differences in growth rates are another factor that may affect the cellular response towards DHA; whether the cells are sensitive or not may depend on whether they are in a proliferative or resting phase. The DHA sensitive (DLD-1 and HCT-8) and less DHA sensitive (LS411N and LS513) cell lines have a doubling time of ~22 h and ~ 40 h, respectively, which also could influence the differences in sensitivity towards DHA. However, the cells were seeded at an optimized cell density to assure both rapid recovery and re-entry to proliferative phase after seeding.

LS411N and LS513 cells used in this thesis are derived from primary carcinoma, while DLD-1 and HCT-8 cells are derived from adenocarcinoma. All four cell lines are derived from different individuals. Hence, the genetic differences could possibly play a role in the observed differences in DHA sensitivity between these four cell lines.

4.2 Gene expression level of autophagy-related genes differ between DHA sensitive and less DHA sensitive cell lines

Gene expression analysis of four CRC cell lines identified significant changes in the expression of 289 probes between DHA sensitive (DLD-1 and HCT-8) and less DHA sensitive (LS411N and LS513) cell lines. The results indicated an association between the expression of genes related to autophagy and DHA sensitivity (table 5). The gene list suggests that the basal level of autophagy may be an important mechanism mediating the cancer cells' response to DHA. Among the genes differentially expressed between DHA sensitive and less DHA sensitive cells were AKT3, DEPTOR, FYN, and PI3KR1 which are known to be involved in the regulation of autophagy.

DEPTOR is an mTOR inhibitor and it's expression is negatively regulated by mTOR. DEPTOR has been found to have antitumor activity in CRC and other cancer types [66, 67]. Ji *et al* (2016) have shown that DEPTOR expression is significantly decreased in tumor tissues of esophageal squamous cell carcinoma (ESCC) patients and predict a poor five-year survival rate. In the same study they found that expression of DEPTOR inhibited the AKT/mTOR pathway and thereby inhibiting proliferation, migration and invasion. These findings indicate that DEPTOR is an important inhibitor in ESCC development and may be used as a potential biomarker to predict prognosis of the patients with esophageal squamous cell carcinoma [68]. In our case this gene was found to be less expressed in the DHA sensitive CRC cells compared to less DHA sensitive cells, indicating the level of DEPTOR as an important regulator of the basal autophagy level in these cells by negatively regulating the AKT/mTOR pathway. A recently published study by our group, showed the results from gene expression level on ten CRC cell lines (DLD-1, HCT-8, LS411N and LS513 cells included), which differed in sensitivity towards DHA treatment [1]. DEPTOR was found among the genes, which correlated with the degree of DHA sensitivity. A study by Yamada *et al* (2016) has shown that the proto-oncogene FYN directly regulates AMPK by phosphorylation, leading to inhibition of AMPK activity and thereby, inhibition of autophagy [69]. This proto-oncogene was found to be highly expressed in DLD-1/HCT-8 cells versus LS411N/ LS513

cells, indicating a lower autophagy level in DLD-1 and HCT-8 cells. Based on these findings, it was interesting to assess the basal autophagy level of the four cell lines.

4.3 The basal level of autophagy is associated with the degree of DHA sensitivity

As mentioned in the introduction, if autophagy is highly accelerated or down regulated, leading to too much or too little autophagy, respectively, the process may act toxic [47]. To determine whether autophagy was associated with DHA sensitivity in CRC cell lines, we first examined the basal level of autophagy using the Cyto- ID marker in the four cell lines. Results showed that the four cell lines have significantly different basal levels of autophagy, that were found to correlate with the degree of DHA sensitivity. The DHA sensitive DLD-1 and HCT-8 cells have lower basal level of autophagy compared to less DHA sensitive LS411N and LS513 cells (fig. 10A). To confirm these findings, the basal level of MAP1LC3BII was assessed by western blotting. MAP1LC3BII is a cellular autophagy marker, and a widely used marker of autophagosomes. The results from western blot showed that the basal level of MAP1LC3BII was higher in the less DHA sensitive LS411N and LS513 cells compared to DHA sensitive DLD-1 and HCT-8 cells. These findings are in accordance with a recently published study by our group, where the basal level of autophagy and basal level of MAP1LC3BII in the ten human CRC cell lines were measured by Cyto-ID and western blot, including DLD-1, HCT-8, LS411N, and LS513 cells [1]. The results showed that the most DHA sensitive cell lines had lower basal level of autophagy. These findings indicated an association between basal level of autophagy and DHA sensitivity.

4.4 Induction of autophagy reduced DHA sensitivity in CRC cells

We suspected that autophagy inducer (rapamycin) and autophagy inhibitor (3-MA) treatments could have an effect on the DHA sensitivity. The DHA-induced growth inhibition in DLD-1 and HCT-8 cells was affected by rapamycin. Rapamycin is a lipophilic macrolide antibiotic, used as an immunosuppressant in organ transplant patients and used to treat autoimmune disorders [70]. The antitumor effect of rapamycin in CRC has been studied *in vivo* and *in vitro* [71]. Rapamycin regulates autophagy by inhibiting mTOR-mediated phosphorylation of Atg13 and ULK1, which is a direct target of mTORC1 [72]. Rapamycin is a well characterized drug that induces autophagy. In this study, we found that rapamycin has some growth inhibitory effect on the DHA sensitive cell lines, DLD-1 and HCT-8, but the effect

was much lower than that of DHA treatment alone. Rapamycin combined with DHA led to a lower growth inhibitory effect than the DHA treatment alone. A possible reason for the decrease of DHA-induced growth inhibition in DLD-1 and HCT-8 cells after the combination treatment with DHA and rapamycin could therefore be an increased level of autophagy.

To further investigate whether differences in the autophagy process could explain the difference in growth reduction between the four cell lines, we assessed the protein level of the biomarker MAP1LC3BII using western blotting, and determined the autophagic flux by using the Cyto-ID probe after exposure to the DHA treatment in the four cell lines. The autophagic flux is characterized by the sequestration of bulk cytoplasm and organelles in double membrane autophagic vesicles and their subsequent degradation by lysosomes [73]. We found that the level of autophagic vacuoles increased when DLD-1 and HCT-8 cells were exposed to DHA treatment, indicating an induction of autophagy. To assess whether the autophagic flux was affected, DLD-1 and HCT-8 cells were treated with DHA combined with rapamycin, and the results indicated that the level of stained autophagic vacuoles was higher compared to DHA and rapamycin treatment alone. These findings are in accordance with findings from western blot showing that the protein level of MAP1LC3BII also increased upon co-treatment with rapamycin and DHA for DLD-1 and HCT-8 cells. These results indicate that DHA-treatment increases the autophagic flux in DLD-1 and HCT-8 cells. Jing *et al* (2011) have shown that autophagy and apoptosis increased simultaneously and induce cell death after DHA treatment in human cervical cancer SiHa cells, human lung cancer (A549) and human breast cancer (MCF-7) [74]. Several studies have shown that patients with different cancer types, including CRC, where the tumor has a high MAP1LC3B expression have higher survival [75]. However, the prognostic relevance of MAP1LC3B expression in CRC has been reported in few studies so far. Yu *et al* (2016) discovered prognostic relevance of MAP1LC3B and Beclin-1 protein in gastric cancer, where a low expression of MAP1LC3B predicted worse prognosis in the gastric cancer patients [76]. Lim *et al* (2017), have reported that DHA increased the expression level of MAP1LC3BII in three glioblastoma cell lines both *in vivo* and *vitro*. *In vivo* experiments were performed using *fat-1* tg mice, implanting GL261 mouse glioma cell line into *fat-1* tg mice and wild type mice. *Fat-1* tg mice express a C. elegans n-3-desaturase, which leads to a significant increase in the n-3 PUFAs/n-6 PUFAs ratio across all organs and tissues. They observed a significant reduction in tumor growth in *fat-1* tg mice. TUNEL assays and MAP1LC3B were measured to determine whether apoptosis and autophagy were related to the inhibition of tumor growth. The results showed that the

amount of both TUNEL-positive cells and the level of MAP1LC3B were higher in the tumor tissue derived from *fat-1* mice compared to the tumor tissue derived from the wild-type mice. These findings suggest growth retardation of GL261 cells by DHA treatment through induction of autophagy [77]. These findings are consistent with our results, giving hope that CRC patients with tumors with low levels of MAP1LC3BII could possibly have positive effect of alternative treatment with DHA in combination with conventional cancer treatment.

4.5 Inhibition of autophagy increased DHA sensitivity

Inhibition of autophagy can increase the efficacy of some anticancer therapies [78]. Based on this, we wanted to investigate whether 3-MA, an autophagy inhibitor, could increase the DHA mediated growth inhibition in the less DHA sensitive cell lines, LS411N and LS513. 3-MA blocks the formation of autophagosomes by controlling class I and class III PI3Ks, and was found to reduce the level of autophagic vacuoles as assessed by the Cyto-ID assay in this study. Results from cell counting showed an increased growth inhibitory effect in LS411N and LS513 cells after co-treatment with DHA and 3-MA. Protein expression analysis showed a slightly decrease in autophagic flux after co-treatment with DHA and 3-MA. In addition, the level of MAP1LC3BII was decreased after co-treatment with DHA and 3-MA in LS411N and LS513 cells, which might suggest that inhibition of autophagy may be involved in the increased DHA sensitivity in these two cell lines.

Interestingly, these findings are consistent with a study monitoring autophagy level in human lung A549 cells by Cyto-ID after exposure to EPA and DHA at different concentrations. They found that co-treatment with 3-MA and DHA caused reduction in the Cyto-ID fluorescence intensity, which are in agreement with our findings [79]. In line with this, a recent study by our group demonstrated that the level of MAP1LC3BII decreased after co-treatment with DHA and 3-MA or chloroquine, which is another autophagy inhibitor. The autophagy level in these cells, was also affected by the same treatment [1].

4.6 DHA treatment affected the AKT signaling pathway in both DHA sensitive and less sensitive CRC cell lines

The gene expression data indicated that the autophagy process and the PI3K/AKT-mTOR pathway could be important to the degree of DHA sensitivity in the CRC cell lines investigated. To further study the mechanism of action during DHA treatment, we studied the

AKT/mTOR signaling pathway. The results showed that p-AKT increased to some extent at early time points in all four cell lines. After 24h, the DHA treatment led to a slight decrease in p-AKT levels in both DHA sensitive cell lines and less DHA sensitive cell lines, indicating that DHA affects this signaling pathway in all four cell lines.

Consistent with the reduction in p-AKT levels for DLD-1 and HCT-8, co-treatment with DHA and rapamycin induced the autophagic flux to a higher level than rapamycin alone, indicated by the results from flow cytometry with cyto-ID probe and western blotting. This indicates that the AKT pathway could be involved in induction of the autophagy process during DHA treatment. Increasing evidence suggest that fatty acid signaling is mediated through the PI3K/AKT pathway [80, 81], and several studies have found that inhibition of the PI3K/AKT/mTOR signaling pathway activates autophagy and induces cell death [82, 83]. In a study by Friedrich *et al* they found that DHA decreased the AKT activity in prostate cancer cells [84].

Another study by Lim *et al* (2016) have examined the effect of DHA exposure on p-AKT level in three glioblastoma cells both *in vitro* and *in vivo*. The results from this study showed that DHA treatment caused a dose-dependent decrease in p-AKT. These findings were confirmed by reduced p-AKT levels in tumor tissue from *fat-1* tg mice, compared with tumor tissue from wild-type mice [77]. Our results from western blot analysis and confocal imaging show that p-AKT levels decreased with DHA and rapamycin treatment alone and even more with co-treatment with DHA and rapamycin in DLD-1 and HCT-8 cells.

Some studies have reported that activation of the PI3K/AKT signaling pathway inhibits autophagy and induces cell death [85, 86]. Results from western blot analysis showed that DHA treatment increased the level of p-AKT in LS411N but not in LS513 cells. However, co-treatment with DHA and 3-MA decreased the p-AKT level in both LS411N and LS513 cells. The total level of AKT seemed to have the same trend as p-AKT but to a much lesser extent. These findings are in the line with a study done by Yao *et al* (2015), who found that n-3 PUFAs induced cell death in the lung cancer A549 cell line, by blocking the autophagic flux. The expression level of p-AKT in this study was significantly increased, indicating that DHA and EPA exerted anti-proliferative and cytotoxic effect on A549 cells [87].

It seems reasonable to speculate that p-AKT should be higher after treatment with 3-MA combined with DHA in LS411N and LS513 cells. Results from western blotting demonstrated

a 3-MA-mediated increase in the level of p-AKT, while co-treatment with DHA and 3-MA decreased the p-AKT level. However, it was observed some problems during western blotting, which could have affected the results. This will be further discussed in chapter 4.8.
In contrast to the western blotting results, confocal imaging showed that DHA treatment increased the expression level of p-AKT in LS411N and LS513 cells. Also, the level of p-AKT increased further with co-treatment with 3-MA and DHA, indicating an activation of the signaling pathway, and a possible mechanism responsible for the DHA-mediated decrease in autophagy. Total AKT level seemed to be unchanged.

4.7 DHA treatment affected the expression level of p-mTOR in different ways in DHA sensitive and less DHA sensitive CRC cell lines

As mentioned in the introduction, AKT plays a key role in the PI3K/mTOR signaling pathway. AKT is phosphorylated by PDK1, and may phosphorylate several protein targets, including mTOR. mTOR is a serine/threonine kinase involved in many signaling pathways that promotes tumor growth. Activated mTOR has been found to be tumor-associated in many cancer tissues [32]. Several studies have shown that PI3K/mTOR signaling is downregulated in many types of cancer, including CRC. Based on the gene expression results indicating differences in the expression level of DEPTOR between DHA sensitive and less DHA sensitive cell lines, we wanted to determine the effect of DHA treatment on mTOR activity in CRC cells. DLD-1 and HCT-8 cells were treated with DHA (70 µM), rapamycin (50 nM) and co-treated with rapamycin and DHA. As hypothesized, both western blotting and confocal imaging results showed that the expression level of p-mTOR in DLD-1 and HCT-8 cells were significantly reduced with co-treatment with DHA and rapamycin compared to rapamycin alone. Its seems reasonable to speculate that the total mTOR should be unchanged for these two cell lines, but it was found to have the same trend as p-mTOR. Kim *et al* (2014) investigated the expression of mTOR in human Non- Small cell lung cancer (NSCLC) after DHA treatment. They found that DHA reduced the levels of p-mTOR in two DHA sensitive NSCLC cell lines. One of these cell lines were treated with rapamycin (1µM) in combination with DHA (30µM) to test the role of mTOR in DHA-induced cell death. They found that DHA induced a reduction in uncleaved PARP and increased the expression level of MAP1LC3BII. This indicates that DHA induced both autophagy and apoptosis, and that this correlated with mTOR inhibition [88]. A recent study by Kim *et al* (2018) showed that DHA induced cell death in glioblastoma cells through suppression of mTOR via AKT inhibition

and AMPK activation both *in vivo* and *in vitro*. These findings indicate the importance of autophagy in antitumor activity of DHA. Reduction in protein levels of p-mTOR and p-AKT, suggest that DHA-induced autophagy is associated with the inhibition of mTOR via downregulation of p-AKT in DLD-1 and HCT-8 cells. Inhibition of mTOR activity has been shown to destroy the balance between pro and anti-apoptotic proteins, thereby improving tumor cell death (reviewed in [32]).

Too high autophagy may promote cell survival by rendering cells resistant to stress, or may cause damage by degrading important components of the cells. The less DHA sensitive LS411N and LS513 cells were exposed to DHA (70µM), 3-MA (3mM) and 3-MA combined with DHA. mTOR activity was measured by western blot analysis and confocal imaging. The results indicated an increased level of p-mTOR after treatment with DHA and a slightly non-significantly decrease in combination with 3-MA and DHA. Yao *et al* (2015) also found that p-mTOR was increased with DHA treatment (152 µM), while the addition of 3-MA decreased the expression level of p-mTOR in lung cancer A549 cells. Their results showed that the total expression level of mTOR was decreased after treatment with DHA combined with 3-MA. Our western blotting results indicated that the total level of mTOR was increased by co-treatment with DHA and 3-MA in LS513, while it seemed to be unchanged in LS411N cells with the same treatment. Since co-treatment with DHA and 3-MA increased the degree of DHA sensitivity in LS411N and LS513 cells, it seems like inhibition of autophagy possibly may improve the anticancer effect of DHA.
Observations from confocal imaging showed that p-mTOR was increased by DHA treatment compared to control in LS411N and LS513 cells. These results indicate that autophagy is inhibited as result of DHA treatment in these cells.

4.8 Troubleshooting the western blotting procedure

It should be noted that during western blotting of mTOR, p-mTOR, AKT and p-AKT we observed that some of the protein bands were partly missing, or had low signals (fig. 25 and 26). To troubleshoot western blotting, others have used specific protocols for detection of large phosphoproteins. When it comes to protein isolation, the lysis buffer did contain phosphatase inhibitors, but the amount could possibly have been increased to better protect the phosphorylated proteins.

Polyacrylamide gel electrophoresis (PAGE) is used to separate desaturated and negatively charged proteins. For high molecular weight proteins like mTOR (289 kDa), a lower concentration gel is recommended to increase the movement of larger proteins. In our case we tested different gel types, both with 4-12% and 3-8% gels, meanwhile it did not improve the signal of the proteins. Kinoshita *et al* have described a protocol for the detection of phosphorylated forms of high molecular weight proteins. In this protocol other gel types, like agarose gel are recommended. Agarose gels are used for very large molecular weight proteins, although, the development of heat may cause the gel to melt during electroblotting [89].

Electroblotting may also have some effect. The choice of pore size is another variable as this will affect the binding of larger or smaller proteins. Proteins are transferred onto polyvinylidene difluoride (PVDF) membranes. PVDF membranes have different pore size and choice of pore size (i.e. 0.45 µm-0.2µm). A 0.2 µm pore size membrane absorbs smaller molecular weight protein, thus we used membrane with a pore size of 0.45 µm for larger proteins. The rate of protein movement is depending on the molecular weight. Therefore, smaller proteins possibly need less time for transfer. In our protocol, the blotting was carried out at 30 voltage (V) for 1.5 h. For protocol for the larger proteins, an increased duration of blotting can improve the transfer of proteins from the acrylamide gel to the membrane. Therefore, we reduced the voltage to 25 V and blotted for 16 h at 4°C. In addition, different transfer buffers with different methanol concentrations were tested. Methanol in the transfer buffer support in stripping the SDS from proteins in SDS-PAGE gels, leading to increase their ability to bind to membrane. However, methanol used in transfer buffer may shrink protein gel and membrane, which may increase the transfer time of large molecular weight proteins with poor solubility in methanol [90].

Different solutions were used to block the membrane. The membrane was blocked first with Oddesy blocking buffer diluted with TBST. We also blocked the membrane with antibody with 5% dry milk. Milk contains several different proteins, one of which is the phosphoprotein, casein. Casein is itself a phosphoprotein and could possibly interfere with phosphorylation level of proteins during western blot. Bovine serum albumin (BSA 5%) are recommended and may give anti-phosphoprotein antibodies [91]. The length of the incubation period with primary antibody is an important factor and may affect the antibody binding to the membrane, especially for large molecular proteins. Therefore, we incubated the primary antibody at 4°C overnight, but it did not improve the results.

One possible variable that may have affected the protein quality, is the freshness/quality of DHA stock. Highly unsaturated lipids, like DHA are readily exposed to oxidation. Factors like oxygen, light and heat contribute to oxidation rates. Antioxidants are known to slow the rate of oxidation and limits the exposure to oxygen [92]. Our DHA stock were stored at -20 °C, but may possibly have been exposed to oxygen during use and storage over time. This could have affected the quality of the proteins separated by western blotting. However, since the results of p-AKT and p-mTOR levels were as expected during the confocal imaging, a potential influence of the quality of the DHA stock seems less likely.

Weak protein signals can also be caused by too low concentration of antibody. However, we have tested different antibody concentration. Furthermore, prolonged washing can decrease the fluorescence signal intensity, but the washing conditions were same in all experiments. Despite the problems with western blotting, the results still represent the mean of three independent experiments.

5. Conclusions and future perspectives

The four human CRC cell lines responded differently to treatment with a physiologically relevant dose of DHA (70 µM). DLD-1 and HCT-8 cells are sensitive to DHA treatment, with a growth inhibitory effect of ~25-45% after 48h. LS411N and LS513 cells responded to a lesser extent to DHA treatment. The results from gene expression analysis, suggest an association between the degree of DHA sensitivity and expression level of genes related to autophagy.

The basal level of autophagy varied between the four studied CRC cell lines. LS411N and LS513 cells with higher DHA tolerance, have a much higher basal autophagy level compared to DLD-1 and HCT-8 cells. The basal protein level of MAP1LC3BII was also higher in LS411N and LS513 cells compared to DLD-1 and HCT-8 cells, indicating a connection between autophagy and DHA sensitivity. Co-treatment with rapamycin reduced the DHA sensitivity in DLD-1 and HCT-8 cells, while the autophagy inhibitor, 3-MA increased the DHA sensitivity in LS411N and LS513 cells. DHA combined with rapamycin treatment increased the level of MAP1LC3BII in DLD-1 and HCT-8 cells compared to rapamycin alone, while co-treatment with DHA and 3-MA decreased the level of MAP1LC3BII in LS411N and LS513 compared to 3-mA alone. The autophagic flux was increased with DHA treatment in DLD-1 and HCT-8 cells, and reduced with DHA treatment in LS411N and LS513 cells.

DHA treatment combined with rapamycin decreased the p-AKT and p-mTOR levels in DLD-1 and HCT-8 cells, suggesting that the DHA-induced autophagy in DLD-1 and HCT-8 cells is possibly regulated by the AKT/mTOR pathway. Confocal imaging indicated that p-AKT and p-mTOR increased in LS411N and LS513 after DHA treatment, while total AKT remained unchanged.

In our recent publication, we suggest that the basal level of autophagy and MAP1LC3BII protein as potential biomarkers for DHA sensitivity in CRC cells. These findings could be confirmed in preclinical animal models in the future. Exome sequencing of cancer cells with different DHA sensitivity could lead to detection of specific genetic patterns and possible discovery of new potential biomarkers for CRC treatment. The PI3K/AKT/mTOR pathway, and other cellular kinases related to autophagy, should be further investigated in regard to DHA sensitivity of CRC cells. Autophagy is an interesting process, both as a mechanism for

cancer prevention and as a target for cancer therapy. High mortality of CRC indicates that the existing cancer treatments in many cases are inadequate. Limitations of chemotherapy could be damage to healthy tissues and lack of specificity. Therefore, it is necessary to improve cancer treatment and more specific cancer therapy is needed. Since development of 5-FU resistance and side effects during treatment, is common, it would be interesting to evaluate the effect of DHA treatment combined with an autophagy inducer or inhibitor in combination with 5-FU treatment both in normal and in cancer cell lines. The synergistic anticancer properties of DHA and 5-FU against CRC cells, would also be interesting to investigate. In addition to cancer cell lines, normal cell lines should also be investigated to make sure whether DHA are toxic only to tumor cells without being cytotoxic to normal cells. However, n-3 PUFAs are normal constituents of the diet and adverse effects of a correct supplementation with these fatty acids seems not likely. Co-treatment with 5-FU and n-3 PUFAs could potentially increase the overall survival rate and quality of life for CRC patients. Next generation sequencing technology, like exome sequencing may give more understanding of CRC genomes, and may lead to the discover of specific gene variants that could indicate which patients that might benefit from DHA supplementation in combination with conventional cancer treatment. Such gene variants could be used as potential biomarkers that may help developing n-3 PUFA based dietary interventions that could form the base for development of personalized diets for CRC patients.

References

1. Samdal, H., et al., *Basal level of autophagy and MAP1LC3B-II as potential biomarkers for DHA-induced cytotoxicity in colorectal cancer cells.* Febs j, 2018.
2. Kremmyda, L., et al., *FATTY ACIDS AS BIOCOMPOUNDS: THEIR ROLE IN HUMAN METABOLISM, HEALTH AND DISEASE - A REVIEW. PART 2: FATTY ACID PHYSIOLOGICAL ROLES AND APPLICATIONS IN HUMAN HEALTH AND DISEASE*, in *Biomed. Pap-Olomouc*. 2011. p. 195-218.
3. Simopoulos, A.P., *Human requirement for N-3 polyunsaturated fatty acids.* Poult Sci, 2000. **79**(7): p. 961-70.
4. Burdge, G., *Alpha-Linolenic acid metabolism in men and women: nutritional and biological implications*. 2004: London :. p. 137-144.
5. Ratnayake, W.M.N. and C. Galli, *Fat and Fatty Acid Terminology, Methods of Analysis and Fat Digestion and Metabolism: A Background Review Paper.* Annals of Nutrition and Metabolism, 2009. **55**(1-3): p. 8-43.
6. Maskrey, B., et al., *Emerging importance of omega-3 fatty acids in the innate immune response: Molecular mechanisms and lipidomic strategies for their analysis*. Vol. 57. 2013.
7. Wiktorowska-Owczarek, A., M. Berezinska, and J.Z. Nowak, *PUFAs: Structures, Metabolism and Functions.* Adv Clin Exp Med, 2015. **24**(6): p. 931-41.
8. Bond, L.M., et al., *Chapter 6 - Fatty Acid Desaturation and Elongation in Mammals*. 2016: Elsevier B.V. 185-208.
9. Rustan, A.C.a.D., C.A. , *Fatty Acids: Structures and Properties. Encyclopedia of Life Sciences, 1-7.* . 2005.
10. Calviello, G., G. Calviello, and S. Serini, *Dietary Omega-3 Polyunsaturated Fatty Acids and Cancer*. 2010, Springer Netherlands.
11. Ghasemi Fard, S., et al., *How does high DHA fish oil affect health? A systematic review of evidence.* Crit Rev Food Sci Nutr, 2018: p. 1-44.
12. Salem, N., Jr. and M. Eggersdorfer, *Is the world supply of omega-3 fatty acids adequate for optimal human nutrition?* Curr Opin Clin Nutr Metab Care, 2015. **18**(2): p. 147-54.
13. *Main conclusions of the NNR 2012*. 2012; Available from: http://www.norden.org/en/theme/former-themes/themes-2016/nordic-nutrition-recommendation/main-conclusions-of-the-nnr-2012/.
14. Russo, G.L., *Dietary n -6 and n -3 polyunsaturated fatty acids: From biochemistry to clinical implications in cardiovascular prevention.* Biochemical Pharmacology, 2009. **77**(6): p. 937.
15. Huerta-Ypez, S., A.B. Tirado-Rodriguez, and O. Hankinson, *Role of diets rich in omega-3 and omega-6 in the development of cancer.* Bolet?n M?dico del Hospital Infantil de M?xico, 2016. **73**(6): p. 446-456.

16. *Cancer*. 2018; Available from: http://www.who.int/mediacentre/factsheets/fs297/en/.
17. *Cancer in Norway*. 2018; Available from: https://www.kreftregisteret.no/Generelt/Fakta-om-kreft/.
18. Lehman, T.A., et al., *ONCOGENES AND TUMOR-SUPPRESSOR GENES.* Environ. Health Perspect., 1991. **93**: p. 133-144.
19. Balkwill, F.R., M. Capasso, and T. Hagemann, *The tumor microenvironment at a glance.* Journal of cell science, 2012. **125**(Pt 23): p. 5591.
20. Hofseth.L.J, W. A., and H. C.C. *Chemical carcinogenesis*. 2017; Available from: https://oncohemakey.com/chemical-carcinogenesis-2/#c023-fig-anc-0001.
21. Hanahan, D. and R.a. Weinberg, *Hallmarks of Cancer: The Next Generation.* Cell, 2011. **144**(5): p. 646-674.
22. *Colorectal cancer statistics*. 2012; Available from: http://www.wcrf.org/int/cancer-facts-figures/data-specific-cancers/colorectal-cancer-statistics.
23. *TYKK- OG ENDETARMSKREFT*. 2016; Available from: https://www.kreftregisteret.no/Generelt/Fakta-om-kreft/Tykk--og-endetarmskreft/.
24. Birt, D.F. and G.J. Phillips, *Diet, Genes, and Microbes.* Toxicologic Pathology, 2014. **42**(1): p. 182-188.
25. Leufkens, A.M., et al., *Diagnostic accuracy of computed tomography for colon cancer staging: a systematic review.* Scand J Gastroenterol, 2011. **46**(7-8): p. 887-94.
26. Li, J., et al., *Inhibition of Autophagy by 3-MA Enhances the Effect of 5-FU-Induced Apoptosis in Colon Cancer Cells.* Annals of Surgical Oncology, 2009. **16**(3): p. 761-771.
27. *Kolorektal cancer*. 2015; Available from: http://legemiddelhandboka.no/Terapi/s%C3%B8ker/+%2Bkolorektal+%2Bkreft/465721.
28. Zhang, Y., Z. Chen, and J. Li, *The current status of treatment for colorectal cancer in China: A systematic review.* Medicine (Baltimore), 2017. **96**(40): p. e8242.
29. Chao, A., et al., *Meat Consumption and Risk of Colorectal Cancer.* JAMA, 2005. **293**(2): p. 172-182.
30. Young, G.P. and R. Le Leu, *Preventing cancer: dietary lifestyle or clinical intervention?* Asia Pac. J. Clin. Nutr., 2002. **11**(sS): p. S618-S631.
31. Skender, B., A.H. Vaculova, and J. Hofmanova, *Docosahexaenoic fatty acid (DHA) in the regulation of colon cell growth and cell death: a review.* Biomed Pap Med Fac Univ Palacky Olomouc Czech Repub, 2012. **156**(3): p. 186-99.
32. D'Eliseo, D. and F. Velotti, *Omega-3 Fatty Acids and Cancer Cell Cytotoxicity: Implications for Multi-Targeted Cancer Therapy.* J Clin Med, 2016. **5**(2).
33. Begum, G., et al., *ER Stress and Effects of DHA as an ER Stress Inhibitor.* Translational Stroke Research, 2013. **4**(6): p. 635.

34. Ameri, K. and A.L. Harris, *Activating transcription factor 4.* International Journal of Biochemistry and Cell Biology, 2008. **40**(1): p. 14-21.
35. Jakobsen, C.H., et al., *DHA induces ER stress and growth arrest in human colon cancer cells: associations with cholesterol and calcium homeostasis * s?* Journal of Lipid Research, 2008. **49**(10): p. 2089-2100.
36. Pettersen, K., et al., *DHA-induced stress response in human colon cancer cells - Focus on oxidative stress and autophagy.* 2016.
37. Yoshida, G.J., *Therapeutic strategies of drug repositioning targeting autophagy to induce cancer cell death: from pathophysiology to treatment.* J Hematol Oncol, 2017. **10**(1): p. 67.
38. González-Polo, R.A., et al., *The Basics of Autophagy*, in *Autophagy Networks in Inflammation*, M.C. Maiuri and D. De Stefano, Editors. 2016, Springer International Publishing: Cham. p. 3-20.
39. Melendez A, B.L., *Autophagy in C. elegans.* 2009.
40. Axe, E.L., et al., *Autophagosome formation from membrane compartments enriched in phosphatidylinositol 3-phosphate and dynamically connected to the endoplasmic reticulum.* J Cell Biol, 2008. **182**(4): p. 685-701.
41. Simonsen, A. and S. Tooze, *Coordination of membrane events during autophagy by multiple class III PI3-kinase complexes*. 2009, Rockefeller University Press: New York. p. 773.
42. Mizushima, N., T. Yoshimori, and Y. Ohsumi, *The Role of Atg Proteins in Autophagosome Formation.* Annual Review of Cell and Developmental Biology, 2011. **27**(1): p. 107-132.
43. Diaz-Troya, S., et al., *The role of TOR in autophagy regulation from yeast to plants and mammals.* Autophagy, 2008. **4**(7): p. 851-65.
44. Barth, S., D. Glick, and K.F. Macleod, *Autophagy: assays and artifacts.* J Pathol, 2010. **221**(2): p. 117-24.
45. Yamada, E. and R. Singh, *Mapping Autophagy on to Your Metabolic Radar*, in *Diabetes*. 2012. p. 272-280.
46. Burada, F., et al., *Autophagy in colorectal cancer: An important switch from physiology to pathology.* World journal of gastrointestinal oncology, 2015. **7**(11): p. 271.
47. Yang, Y.P., et al., *Molecular mechanism and regulation of autophagy.* Acta Pharmacol Sin, 2005. **26**(12): p. 1421-34.
48. Martini, M., et al., *PI3K/AKT signaling pathway and cancer: an updated review.* Annals of Medicine, 2014. **46**(6): p. 372-383.
49. Porta, C., C. Paglino, and A. Mosca, *Targeting PI3K/Akt/mTOR Signaling in Cancer.* Frontiers in oncology, 2014. **4**: p. 64.
50. *PI3K / Akt Signaling Interactive Pathway*. 2007; Available from: https://www.cellsignal.com/contents/science-cst-pathways-pi3k-akt-signaling-resources/pi3k-akt-signaling-interactive-pathway/pathways-akt-signaling.

51. Sarbassov, D.D., et al., *Phosphorylation and Regulation of Akt/PKB by the Rictor-mTOR Complex.* Science, 2005. **307**(5712): p. 1098-1101.
52. Wu, Y.-T., et al., *Dual role of 3-methyladenine in modulation of autophagy via different temporal patterns of inhibition on class I and III phosphoinositide 3-kinase.* The Journal of biological chemistry, 2010. **285**(14): p. 10850.
53. Vara, J.n.F., et al., *PI3K/Akt signalling pathway and cancer.* Cancer Treatment Reviews, 2004. **30**(2): p. 193-204.
54. Carnero, A., et al., *The PTEN/PI3K/AKT signalling pathway in cancer, therapeutic implications.* Curr Cancer Drug Targets, 2008. **8**(3): p. 187-98.
55. Heras-Sandoval, D., et al., *The role of PI3K/AKT/mTOR pathway in the modulation of autophagy and the clearance of protein aggregates in neurodegeneration.* Cellular Signalling, 2014. **26**(12): p. 2694-2701.
56. Bai, X. and Y. Jiang, *Key factors in mTOR regulation.* Cellular and Molecular Life Sciences, 2010. **67**(2): p. 239-253.
57. Kim, Y. and K. Guan, *mTOR: a pharmacologic target for autophagy regulation*, in *J. Clin. Invest.* 2015. p. 25-32.
58. Peterson, T.r., et al., *mTOR Complex 1 Regulates Lipin 1 Localization to Control the SREBP Pathway.* Cell, 2011. **146**(3): p. 408-420.
59. Shaw, R.J., *LKB1 and AMP?activated protein kinase control of mTOR signalling and growth*. 2009: Oxford, UK. p. 65-80.
60. Sabatini, D.M., *mTOR and cancer: insights into a complex relationship.* Nature Reviews Cancer, 2006. **6**: p. 729.
61. Lum, J.J., R.J. DeBerardinis, and C.B. Thompson, *Autophagy in metazoans: cell survival in the land of plenty.* Nature Reviews Molecular Cell Biology, 2005. **6**: p. 439.
62. Huang, S. and F.A. Sinicrope, *Celecoxib-induced apoptosis is enhanced by ABT-737 and by inhibition of autophagy in human colorectal cancer cells.* Autophagy, 2010. **6**(2): p. 256-69.
63. Seglen, P.O. and P.B. Gordon, *3-Methyladenine: specific inhibitor of autophagic/lysosomal protein degradation in isolated rat hepatocytes.* Proc Natl Acad Sci U S A, 1982. **79**(6): p. 1889-92.
64. Noding, R., et al., *Effects of polyunsaturated fatty acids and their n-6 hydroperoxides on growth of five malignant cell lines and the significance of culture media.* Lipids, 1998. **33**(3): p. 285-93.
65. Maehle, L., et al., *Effects of n-3 fatty acids during neoplastic progression and comparison of in vitro and in vivo sensitivity of two human tumour cell lines.* Br J Cancer, 1995. **71**(4): p. 691-6.
66. Obara, A., et al., *DEPTOR-related mTOR suppression is involved in metformin's anti-cancer action in human liver cancer cells.* Biochem Biophys Res Commun, 2015. **460**(4): p. 1047-52.

67. Lai, E.Y., et al., *DEPTOR expression negatively correlates with mTORC1 activity and tumor progression in colorectal cancer.* Asian Pac J Cancer Prev, 2014. **15**(11): p. 4589-94.
68. Ji, Y.M., et al., *DEPTOR suppresses the progression of esophageal squamous cell carcinoma and predicts poor prognosis.* Oncotarget, 2016. **7**(12): p. 14188-98.
69. Yamada, E., et al., *Fyn phosphorylates AMPK to inhibit AMPK activity and AMP-dependent activation of autophagy.* Oncotarget, 2016. **7**(46): p. 74612-74629.
70. Lamming, D.W., et al., *Rapalogs and mTOR inhibitors as anti-aging therapeutics.* J Clin Invest, 2013. **123**(3): p. 980-9.
71. Gulhati, P., et al., *Targeted inhibition of mammalian target of rapamycin signaling inhibits tumorigenesis of colorectal cancer.* Clin Cancer Res, 2009. **15**(23): p. 7207-16.
72. Wang, X.W. and Y.J. Zhang, *Targeting mTOR network in colorectal cancer therapy.* World J Gastroenterol, 2014. **20**(15): p. 4178-88.
73. Fukui, M., et al., *EPA, an omega-3 fatty acid, induces apoptosis in human pancreatic cancer cells: Role of ROS accumulation, caspase-8 activation, and autophagy induction.* Journal of Cellular Biochemistry, 2013. **114**(1): p. 192-203.
74. Jing, K., et al., *Docosahexaenoic acid induces autophagy through p53/AMPK/mTOR signaling and promotes apoptosis in human cancer cells harboring wild-type p53.* Autophagy, 2011. **7**(11): p. 1348-1358.
75. Wu, W.Y., et al., *Clinical significance of autophagic protein LC3 levels and its correlation with XIAP expression in hepatocellular carcinoma.* Med Oncol, 2014. **31**(8): p. 108.
76. Yu, S., et al., *Low expression of MAP1LC3B, associated with low Beclin-1, predicts lymph node metastasis and poor prognosis of gastric cancer.* Tumour Biol, 2016. **37**(11): p. 15007-15017.
77. Kim, S., et al., *?3-polyunsaturated fatty acids induce cell death through apoptosis and autophagy in glioblastoma cells: In vitro and in vivo.* Oncology Reports, 2018. **39**(1): p. 239-246.
78. Choi, K., et al., *A Review of Fundamentals of Statistical Concepts in Clinical Trials.* J Korean Soc Clin Pharmacol Ther, 2012. **20**(2): p. 109-124.
79. Zajdel, A., A. Wilczok, and M. Tarkowski, *Toxic effects of n-3 polyunsaturated fatty acids in human lung A549 cells.* Toxicology in Vitro, 2015. **30**(1, Part B): p. 486-491.
80. Couplan, E., et al., *Polyunsaturated fatty acids inhibit PI3K activity in a yeast-based model system*. Vol. 4. 2009. 1190-1197.
81. Wan, M., et al., *Eicosapentaenoic acid inhibits TNF-α-induced Lnk expression in human umbilical vein endothelial cells: involvement of the PI3K/Akt pathway.* The Journal of Nutritional Biochemistry, 2007. **18**(1): p. 17-22.
82. Wang, L., et al., *Blocking autophagic flux enhances matrine-induced apoptosis in human hepatoma cells.* Int J Mol Sci, 2013. **14**(12): p. 23212-30.

83. Xie, X., E.P. White, and J.M. Mehnert, *Coordinate autophagy and mTOR pathway inhibition enhances cell death in melanoma.* PLoS One, 2013. **8**(1): p. e55096.
84. Friedrichs, W., et al., *Omega-3 fatty acid inhibition of prostate cancer progression to hormone independence is associated with suppression of mTOR signaling and androgen receptor expression.* Nutr Cancer, 2011. **63**(5): p. 771-7.
85. Surviladze, Z., et al., *Cellular entry of human papillomavirus type 16 involves activation of the phosphatidylinositol 3-kinase/Akt/mTOR pathway and inhibition of autophagy.* J Virol, 2013. **87**(5): p. 2508-17.
86. El-Khoury, V., et al., *Disruption of autophagy by the histone deacetylase inhibitor MGCD0103 and its therapeutic implication in B-cell chronic lymphocytic leukemia.* Leukemia, 2014. **28**(8): p. 1636-46.
87. Yao, Q., et al., *Role of autophagy in the omega-3 long chain polyunsaturated fatty acid-induced death of lung cancer A549 cells.* Oncol Lett, 2015. **9**(6): p. 2736-2742.
88. Kim, N., et al., *Docosahexaenoic Acid Induces Cell Death in Human Non-Small Cell Lung Cancer Cells by Repressing mTOR via AMPK Activation and PI3K/Akt Inhibition.* BioMed Research International, 2015. **2015**.
89. Kinoshita, E., E. Kinoshita-Kikuta, and T. Koike, *Separation and detection of large phosphoproteins using Phos-tag SDS-PAGE.* Nat Protoc, 2009. **4**(10): p. 1513-21.
90. *Western Blotting Transfer Methods*. Available from: https://www.thermofisher.com/no/en/home/life-science/protein-biology/protein-biology-learning-center/protein-biology-resource-library/pierce-protein-methods/western-blot-transfer-methods.html#blotting.
91. J., B.J., et al., *An overview of technical considerations for Western blotting applications to physiological research.* Scandinavian Journal of Medicine & Science in Sports, 2017. **27**(1): p. 4-25.
92. Adam, I., et al., *Oxidation in EPA- and DHA-rich oils: an overview.* Lipid Technology, 2016. **28**(3-4): p. 55-59.

Appendix

Appendix A: Chemicals and equipment

Cell cultivation:

- Cell cultivation flasks (75 cm^2 and 175 cm^2), Costar (USA)
- 6 and 12 well plates, Costar (USA).
- Tissue Culture dish, 150 x 20 mm, SPL Lifescience Co, Ltd (Korea)
- Clinical tube, 50 ml (USA)
- Cellstar tubes, 15 ml, greiner bio-one
- Costar Serological Pipettes (1ml, 5ml, 10, ml 25ml), Costar (USA)
- RPMI 1640 Medium, Gibco (England)
- Fetal bovine serum (FBS), Gibco (England)
- Phosphate buffered saline (PBS), Oxoid (England)
- Trypsin solution (0.25 %) with EDTA (0.02%), Lonza (Belgium)
- Gentamicin, 10mg/ml), Gibco (England)

Treatments

- Docosahexaenoic acid (DHA, 25 µg in 200 µL EtOH), (Sigma)
- Ethanol (Absolute alcohol prima), Arcus (Oslo, Norway)
- 3-Methyladenine (3-MA, Sigma, M9281)
- Rapamycin (50 nM) (Santa Cruz Biotechnology (Dallas, Texas, USA), product nr sc-3504 (CAS 53123-88-9))
- DMSO (50nM) (Cat.NO D2660-100ML. Lot# RNBF4514, UK)

Imaging:

- Axiovert 200 microscope with confocal module LSM 510 Meta and a 63x1.4 W objective (Carl Zeiss)
- Zeiss LSM Image Examiner Software version 4.2.0.121

Protein isolation:

- EDTA (1M), Sigma-Aldrich (USA)
- Biorad protein assay dye reagent concentrate, Bio-Rad laboratories (USA)

Western blotting:

- NuPAGE Bis-Tris gels, Life Technologies (USA)
- NuPAGE MOPS Running buffer, Life Technologies (USA)
- NuPAGE transfer buffer, Life Technologies (USA)
- XCell Mini-Cell, Life Technologies (USA)
- XCell II Blot Module, Life Technologies (USA)
- PDVF membrane, Millipore (USA)
- Odyssey^{R} protein molecular weight marker, 928-40000, LI-COR biosciences (USA)

Flow Cytometry:

- BD FACSCanto, VWR international (USA)
- Cyto-ID autophagy detecton kit: ENZ-51031-K200, ENZO life sciences (USA)

Appendix B: Buffers and solutions used during protein isolation and western blotting

NuPAGE MOPS Running Buffer (1 L)

- 50 mL 20xNuPAGE MOPS running buffer
- 950 mL dH2O

NuPAGE Transfer Buffer (1 L)

- 850 mL dH2O
- 100 mL methanol
- 50 mL NuPAGE Transfer Buffer

Phosphate buffered saline (PBS) washing buffer (1 L)

- 1 L dH2O
- 20 PBS tablets
- (Add 10 mL Tween20 to make PBST)

10xTris-buffered saline (TBS)

- 200 mM (0.2 mol/L) Tris (hydroxymethyl)-aminomethane
- 1369 mM (1.369 mol/L) NaCl

- Making 1 L
- Mix 900 mL dH2O, 24.2 g Tris(hydroxymethyl)-aminomethan and 80 g NaCl. Adjust the pH to 7.6 by using concentrated HCl or NaOH. Add dH2O to get a total volume of 1 L.

Tris-buffered saline (TBS) washing buffer (1 L)

- 100 mL 10xTBS
- 900 mL dH2O
- (Add 10 mL Tween20 to make TBST)

Dry milk blocking buffer:

- 5 g Blotting Grade Blocker Non-fat Dry milk (5%) ()
- 100 mL TBST/PBST (when detecting phosphorylated or phosphorylated epitopes, respectively).

Primary- and secondary antibody solution:

- Dry milk blocking buffer + primary/secondary antibody in appropriate dilution

Lysis buffer for isolation of total cell protein extracts (500 µl):

- 400 µL 8M urea-buffer with Triton-x (0,24g Urea, 5µl Triton, 395 µl MQ water)
- 50 µl DTT
- 10 µl PIC2
- 10 µl PIC3
- 25 µl PI /Complete

Appendix C: Protein ladders

Picture: Odyssey protein molecular weight marker, 928-40000(LI-COR biosciences)

Appendix D: Buffers and antibody solutions during immunofluorescent staining

Blocking buffer

- 3% Goat serum
- 97% 1xPBS

Primary/secondary antibody solution

- 1% Goat serum
- 99% 1xPBS
- Primary/ secondary

Appendix E: Buffers and solutions used during flow cytometry

Cyto-ID 1x Assay buffer (10 mL):

- 1 mL 10 x Assay buffer
- 9 ml MQ

Cyto-ID Green detection reagent (1 mL)

- 1 µL green detection reagent
- 1 mL 1 x Assay buffer